IDEA

Innovations Deserving Exploratory Analysis Programs

Highway IDEA Program

Application of Shape Memory Alloys in Seismic Rehabilitation of Bridges

Final Report for Highway IDEA Project 91

Prepared by:
Reginald DesRoches, Georgia Tech, Atlanta, GA

August 2005

TRANSPORTATION RESEARCH BOARD
OF THE NATIONAL ACADEMIES

INNOVATIONS DESERVING EXPLORATORY ANALYSIS (IDEA) PROGRAMS
MANAGED BY THE TRANSPORTATION RESEARCH BOARD (TRB)

This NCHRP-IDEA investigation was completed as part of the National Cooperative Highway Research Program (NCHRP). The NCHRP-IDEA program is one of the four IDEA programs managed by the Transportation Research Board (TRB) to foster innovations in highway and intermodal surface transportation systems. The other three IDEA program areas are Transit-IDEA, which focuses on products and results for transit practice, in support of the Transit Cooperative Research Program (TCRP), Safety-IDEA, which focuses on motor carrier safety practice, in support of the Federal Motor Carrier Safety Administration and Federal Railroad Administration, and High Speed Rail-IDEA (HSR), which focuses on products and results for high speed rail practice, in support of the Federal Railroad Administration. The four IDEA program areas are integrated to promote the development and testing of nontraditional and innovative concepts, methods, and technologies for surface transportation systems.

For information on the IDEA Program contact IDEA Program, Transportation Research Board, 500 5th Street, N.W., Washington, D.C. 20001 (phone: 202/334-1461, fax: 202/334-3471, http://www.nationalacademies.org/trb/idea)

Acknowledgements

I would like to acknowledge Dr. Subhash Gupta and Dr. Frank Scerzine at Special Metals Corporation for their generous donations of material and their advice in regards to the material processes and properties of Nitinol used in the study.

Table of Contents

Executive Summary

Recent earthquakes in the United States and Japan have highlighted the vulnerability of bridges to moderate and strong ground motion. During the 1995 Kobe earthquake, 60% of all bridges in the city were damaged, with a total cost estimated at over 10 billion US dollars for their repair. Significant damage to bridges also occurred in the 1994 Northridge and 1989 Loma Prieta earthquakes. A major problem in all three earthquakes was excessive movement at the hinges due to bearing and restrainer failure. Recent earthquakes have shown that conventional hinge restrainers used in the United States and Japan do not provide adequate protection from unseating, which can lead to collapse of bridges. The research program evaluated the efficacy of using superelastic shape memory alloy restrainers to reduce the seismic vulnerability of bridges due to unseating. The study consisted of materials testing, detailed analytical studies, large-scale shake table tests, and cost analysis.

Shape-memory alloys (SMA) are a class of alloys that display several unique characteristics, including Young's modulus-temperature relations, shape memory effects, and high damping characteristics. In most current applications, the temperature-induced phase change characteristic of shape-memory alloys is used. For some SMA, such as Nitinol (NiTi SMA), the phase change can be stress-induced at room temperature if the alloy has the appropriate formulation and treatment. Passive energy dissipation devices using shape-memory alloys have taken advantage of the high damping characteristics of these devices. The research investigated using SMA restrainer rods and cables to dissipate energy and recenter at the intermediate hinges in a bridge. The restrainers have multiple roles. First, they can limit the relative displacement between frames, thereby reducing the risk of collapse due to unseating of frames at the hinge. Second, by concentrating energy dissipation in controlled locations, these devices can be used to reduce the demand on individual frames in a multiple-frame bridge, thereby enhancing the performance of these structures.

Experimental tests of SMA bars and wires provided detailed information on the force-displacement relationships, recentering capability, affects of loading frequency, temperature, and material size on the strength of the devices. Analytical studies have been performed, based on experimental results of the SMA restrainers. The analytical studies illustrate that SMA rods may be very effective in limiting hinge displacement in bridges. The energy dissipation characteristics help reduce the displacements in bridges due to earthquake loads 25-50% more than conventional steel cable restrainers.

A ¼-scale bridge test was performed in the laboratory to assess the performance of SMA-based restrainer devices. The device showed that SMAs are very effective in limiting displacements in bridges, and validated the results of previous analytical studies.

A detailed cost analysis showed that while SMA restrainer cables are slightly (approximately 13%) more expensive compared to traditional steel restrainer cables, the improvement in bridge performance may warrant the increased cost. Also, when considering life-cycle costs, and the cost to replace damaged steel restrainer cables, the use of SMA restrainer cables may be a more cost-effective option.

IDEA Product

This project research evaluated the effectiveness of restraining devices made of shape memory alloys that can be applied to retrofit of bridges. By concentrating energy dissipation in controlled locations, and having recentering capability, the these devices can be used to reduce the demand on individual frames in a multiple-frame bridge, thereby enhancing the performance of these structures.

Background on Shape Memory Alloys

Shape memory alloys are a class of alloys that display several unique characteristics, including Young's modulus-temperature relations, shape memory effects, and high damping characteristics. Unlike plastically deforming metals, the nonlinear deformation is reversible. This unique "shape memory" characteristic is a result of a martensitic phase-change that can be temperature induced or stress-induced as shown in Figure 1a. Stress-induced transformation leads to a superelastic (or pseudo-elastic) property, as shown in Figure 1a. Superelastic shape memory alloys possess several characteristics that make them desirable for use as restrainers and passive energy dissipation devices in bridges. These characteristics include: (1) hysteretic damping; (2) highly reliable energy dissipation based on a repeatable solid state phase transformation; (3) excellent low- and high-cycle fatigue properties; and (4) excellent corrosion resistance. The stress-strain relationship is characterized by an elastic region, a long horizontal plateau, followed by a significant increase in stiffness. This increase in stiffness at high strains is an ideal property for limiting displacements at hinges due to very large excitation, such as that from near field motions. Upon unloading, the material returns to the origin with little permanent offset. Table 1 shows a comparison of the properties of shape memory alloys and structural steel.

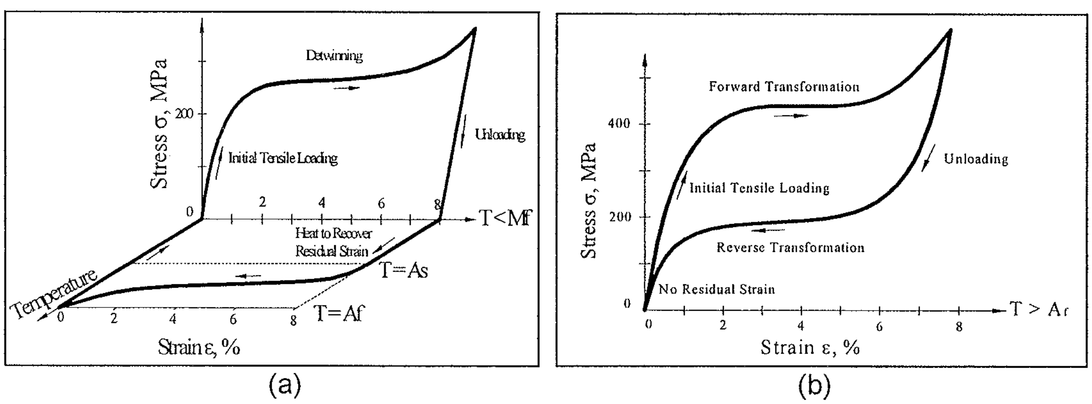

Figure 1. Stress-strain plots for SMAs exhibiting the shape memory effect (a) and the super-elastic effect (b)

While SMA's have been commercially available since the 1960s, their application has been limited. It is only in the past 20 or so years that the material has found functional applications in aerospace, marine, and biomedical fields (Van Humbeeck, 1992; Van Humbeeck, 1999). The growth in materials research revealed the potentials as well as the limitations of SMA's. An improvement in quality and reliability combined with a significant decrease in prices has led to new potential applications for the material and the redressing of applications that were previously deemed unfeasible.

Properties	NiTi SMA Austenite	NiTi SMA Martensite	Steel
Young's Modulus	30-85 GPa	20-40 GPa	200 GPa
Yield Strength	195-700 MPa	70-140 MPa	250-520 MPa
Ultimate Tensile Strength	800-2000 MPa		500-900 MPa
Recoverable Elongation	6-8% typically		0.2%
Elongation to Failure	~25% (up to 50%)		20%
Machinability	Difficult		Good
Corrosion Resistance	Excellent		Fair

Table 1. Properties of NiTi shape memory alloys in comparison to typical structural steel.

Many current applications take advantage of the temperature-induced phase change characteristic of shape memory alloys. For some SMA's, such as Nitinol (NiTi SMA), the phase change can be stress-induced at room temperature if the alloy has the appropriate formulation and treatment, as shown in Figure 2 below. Passive energy dissipation devices using shape-memory alloys have taken advantage of the high damping characteristics of these devices. There have been several studies of applications for NiTi SMA's to seismic resistant design.

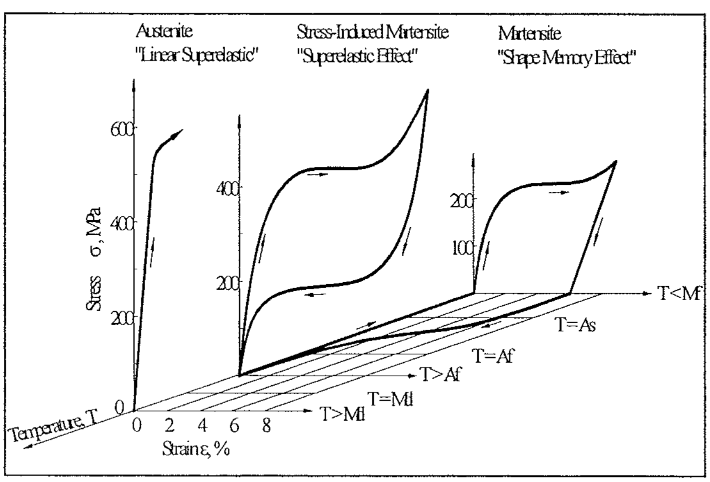

Figure 2. Thermomechanical nature of NiTi

The shortcomings of traditional unseating prevention devices can potentially be addressed with the use of shape memory alloy – based restrainers. They have the ability to dissipate significant energy through repeated cycling without significant degradation or permanent deformation. Their usable strain range is on the order of 7-9%, which provides very high energy dissipation per unit mass of material. The material has excellent low and high cycle fatigue properties, and excellent corrosion resistance. The damping properties are largely amplitude and frequency independent, which is particularly useful for response to multi-frequency, variable amplitude earthquake ground motion records. The proposed research will evaluate the efficacy of SMA-based restrainers in bridges. The restrainers will serve multiple roles. First, they can limit the relative displacement between frames, thereby reducing the risk of collapse due to unseating of frames at the hinges. Second, by concentrating energy dissipation in controlled locations, these "restrainers" will serve as dampers, which will reduce the demand on individual frames in a multiple frame bridge. Finally, they provide a fail-safe mechanism during response to large near-field ground motion.

Investigation of Ternary alloys doped with Cr or Fe

NiTiCr, and NiTiFe alloys are tested to evaluate the possibility of using ternary alloys, instead of the binary NiTi alloy. The recommendations from these results are that the binary form of SMAs (NiTi) exhibited superior performance compared with the Ternary NiTiCr or NiTiFe. In particular, the NiTiFe did not exhibit the superelastic behavior that is characteristic of NiTi.

NiTiCr

The research focused on the cyclic characteristics of NiTiCr. The specimens were composed of 55.73% Ni, 44.04% Ti, and 0.23% Cr by weight. Several 0.085" diameter, 6.5" length, 2.5" gauge length superelastic wires were annealed at 400° C, 500° C, and 600° C for 15 minutes and water quenched. They were then tested quasi-statically (0.025 Hz) using a MTS 810 material testing system fitted with custom wire grips. From the stress-strain plots obtained, it was determined that the specimens annealed at 400° C displayed the best super-elastic qualities (Figure 3).

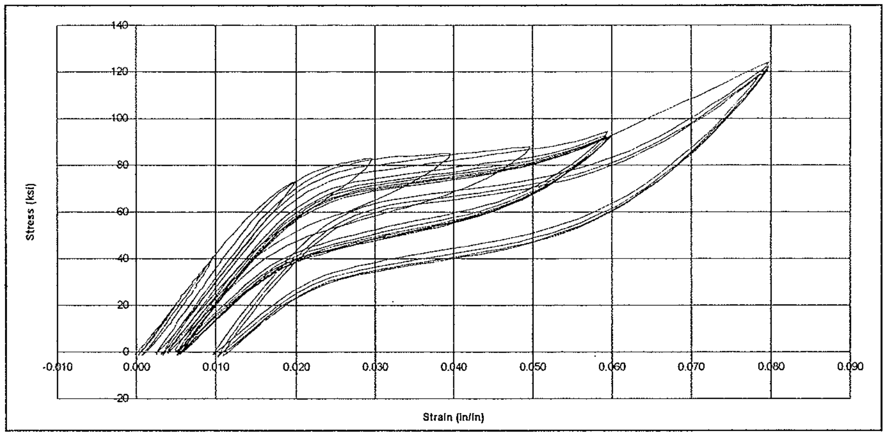

Figure 3. NiTiCr quasi-static strain control - 400° C

More NiTiCr specimens having the same diameter, length, and gauge length were annealed at 400° C and tested dynamically at 0.5 Hz, 1 Hz, and 2 Hz. It was observed that residual stresses after unloading increase successively with each cycle. The initial modulus of elasticity was found to be 4350 ksi, and the yield strength obtained was 64 ksi. When the specimens were strained at 6%, the residual strain was approximately 1%. The equivalent viscous damping - ξ_{eq} was calculated for all specimens (Figure 4).

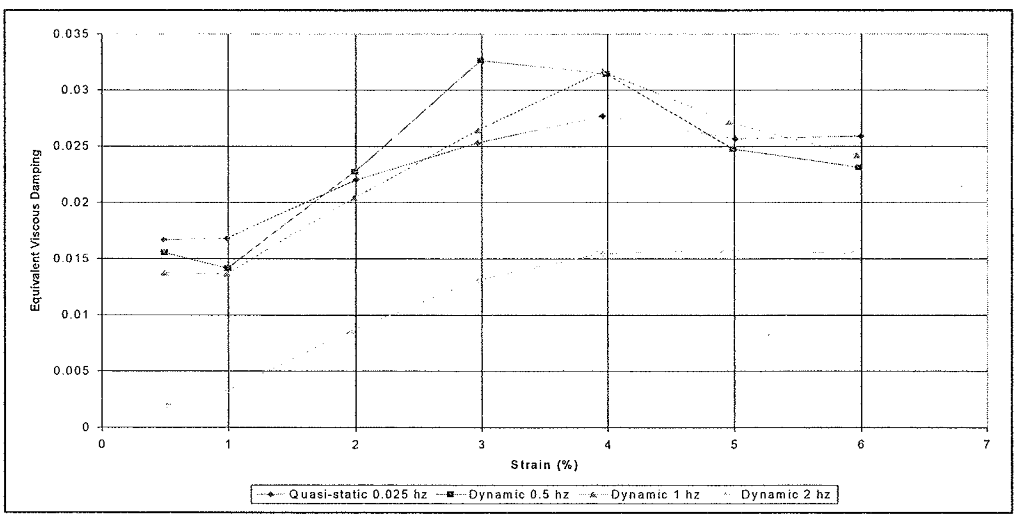

Figure 4. Equivalent viscous damping ξ_{eq} – NiTiCr

NiTi

NiTi wires composed of 56.05% Ni and 43.95% Ti by weight were used for these tests. The specimens measured 0.071" (1.8 mm) in diameter, and 5.9" (150 mm) in length, with a gauge length of 2.5" (63.5 mm). They were annealed at 350° C for 30 minutes and water quenched. They were then tested quasi-statically (0.025 Hz), at 0.5 Hz, 1 Hz, and 2 Hz. Figure 5 shows the stress-strain plots for the NiTi specimen tested at 0.025 Hz.

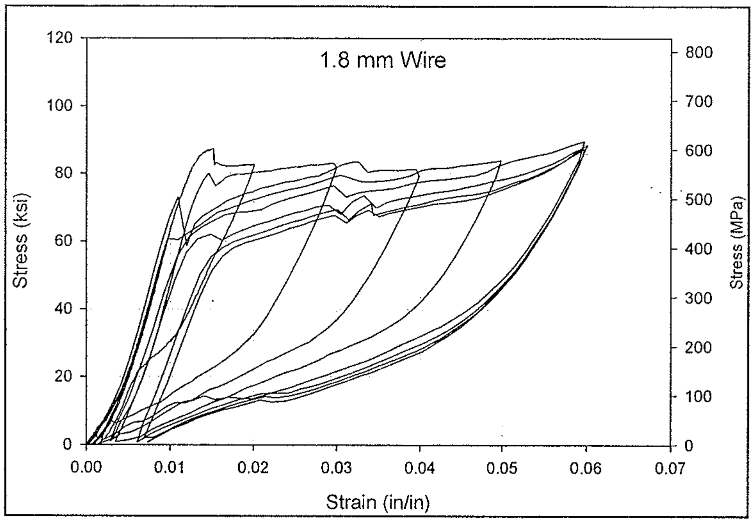

Figure 5. Stress-strain behavior – quasi static test – NiTi

It was observed that residual stresses after unloading increase successively with each cycle. The initial modulus of elasticity was found to be 5802 ksi (40,000 MPa), and the yield strength obtained was 79.8 ksi (557 MPa). When the specimens were strained at 6%, the residual strain was approximately 0.73%. The equivalent viscous damping (ξ_{eq}) was calculated for all specimens and is shown on Figure 6.

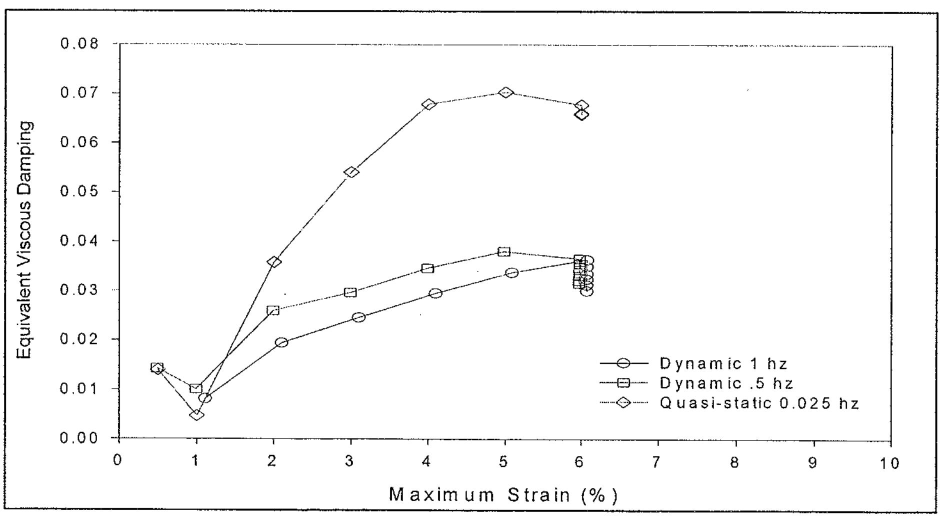

Figure 6. Equivalent viscous damping ξ_{eq} – NiTi

NiTiFe

NiTiFe wires composed of 51.95% Ni, 44.71% Ti, and 3.43% Fe (by weight) were tested. The specimens had a diameter of 0.85" (21.6 mm), a length of 6.5" (165 mm), and a gauge length of 2.5" (63.5 mm). These specimens were annealed at 400° C for 30 minutes and water quenched. After subjecting the specimens to a 0.025 Hz quasi-static test, the stress-strain behavior showed that the material was not behaving in a superelastic manner. Therefore, no more tests were done on the material, and the superelastic properties were not calculated. The stress-strain plot of NiTiFe tested quasi-statically is shown on Figure 7. The equivalent viscous damping - ξ_{eq} was calculated for this specimen and is shown on Figure 8.

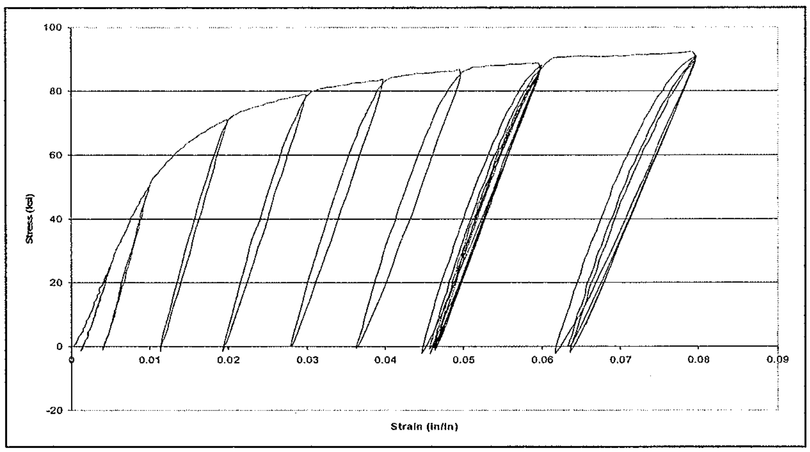

Figure 7. Stress-strain behavior – NiTiFe

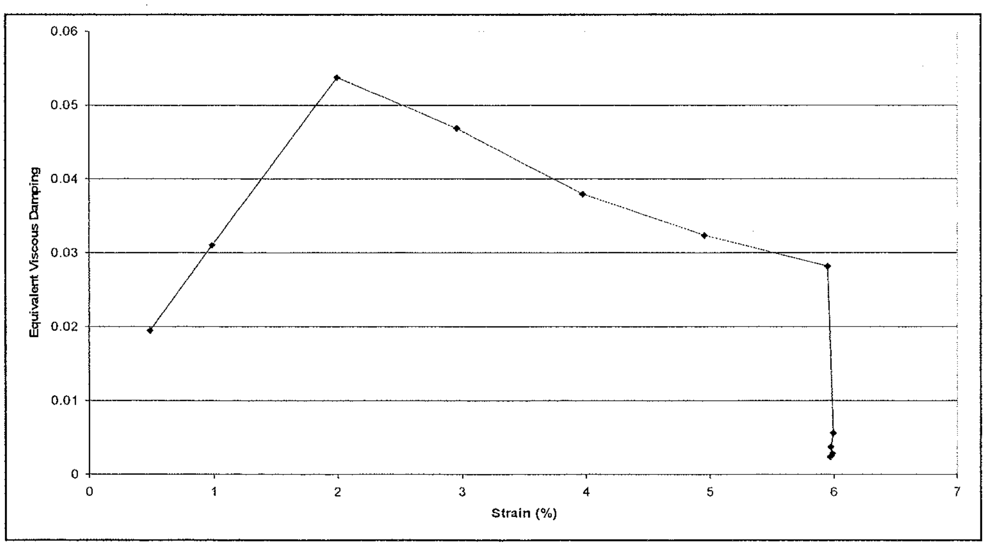

Figure 8. Equivalent viscous damping ξ_{eq} – NiTiFe

Detailed Investigation of the Mechanical Behavior of Ternary NiTiCr and NiTi SMAs

Given the previous findings which showed the inefficiency of ternary NiTiFe shape memory alloys as a recentering device, this stage of the study focused on a detailed comparison between the mechanical behavior of NiTiCr and NiTi under loadings typical of a seismic event. Contained are the results of an in depth annealing study and strain rate study of NiTiCr and NiTi each from a single batch of material in order to eliminate any compositional effects associated with the materials behavior. The results provide evidence into the proper annealing temperature for both NiTiCr and NiTi to ensure the least amount of residual strain during cycling and thus providing the greatest recentering capability. This limits the hinge opening when used as restrainer cables for seismic rehabilitation in bridge systems. Further, the stress-strain behavior was obtained for both the ternary and binary SMAs undergoing a far field type loading protocol at strain rates of 0.5 Hz, 1.0 Hz, and 2.0 Hz. The results show a decrease in the residual strain with increased strain rate. Both types of SMAs also provided damping through their superelastic behavior.

Annealing Study

The research focused on the cyclic characteristics of both NiTiCr and NiTi shape memory alloys. The NiTiCr specimens contained 0.25 wt % of Cr and are 40% cold worked resulting in a diameter of 0.085" (2.16 mm). The specimens have an austenite start temperature of -20°C assuring superelastic behavior at room temperature. The NiTi specimens are near equiatomic and are 40% cold worked resulting in a diameter of 0.085" (2.16 mm). All specimens are cut to a length of 6.5" (165.1 mm) for testing. A MTS hydraulic testing apparatus is used to perform the cyclic tensile tests under strain control. Strains are measured using a 1-inch gauge length extensometer and the loads are measured with the internal load cell of the actuator.

Although previous annealing tests had been conducted, more detailed further testing was necessary in order to conclude the proper annealing temperatures for both NiTiCr and NiTi in order to provide the smallest residual strains. The annealing temperatures that were studied for the NiTiCr specimens were 300°C to 500°C at intervals of 50°C and for the NiTi specimens the annealing temperatures studied were 300°C to 450°C at intervals of 50°C. These temperatures were chosen based on previous results. The NiTiCr specimens were annealed for 15 minutes while the NiTi specimens were annealed for 30 minutes and both were immediately water quenched after annealing was completed. For each temperature, three specimens were tested and the average value of the equivalent viscous damping and residual strain were studied. The residual strain results for the NiTiCr and NiTi specimens can be found in Figure 9 and Figure 10 respectively.

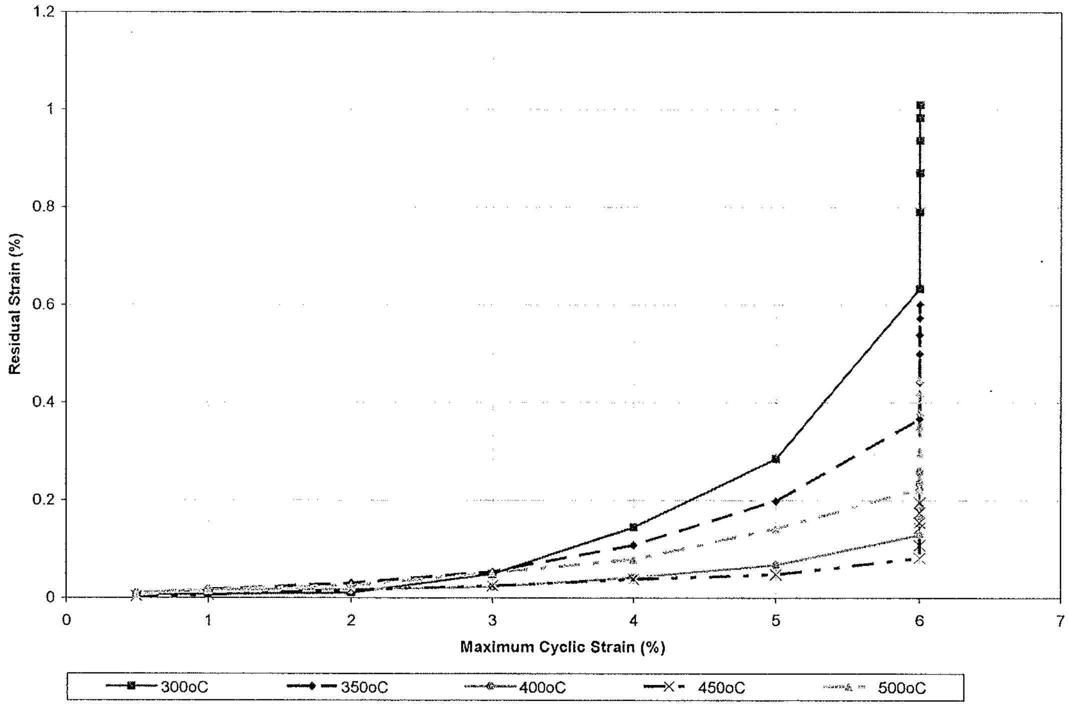

Figure 9. NiTiCr average residual strain per maximum cyclic strain cycled at 0.025 Hz

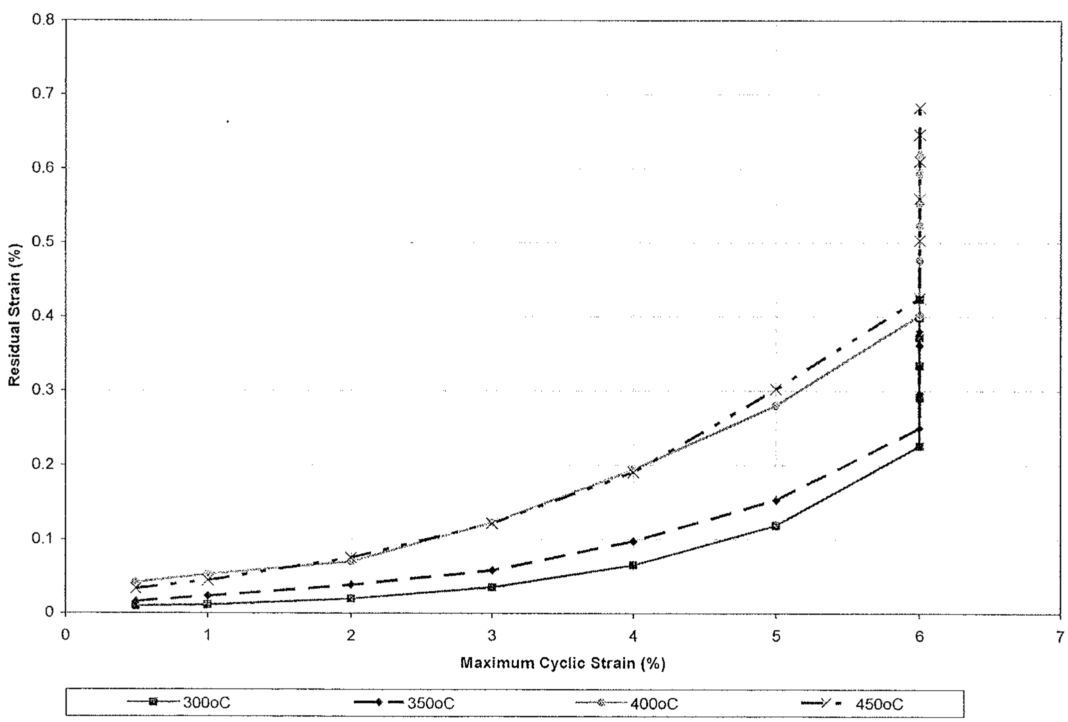

Figure 10. NiTi average residual strain per maximum cyclic strain cycled at 0.025 Hz

The results clearly show that for the NiTiCr specimens, annealing at 450°C provides the lowest amount of residual strain. After undergoing six 6% strain cycles, the residual strain was approximately 0.2% showing good recentering capability even at large strain levels. Upon inspection of the NiTi results, annealing at 300°C results in the smallest values of residual strain up to the second 6% strain cycle at which point the residual strain for the specimen that was annealed at 350°C has a smaller residual strain value. The residual strain values after six 6% strain cycles were approximately 0.42% and 0.40% for the specimens annealed at 300°C and 350°C, respectively. Since it is expected that SMA restrainer cables will undergo several cycles of large strain values during a seismic event, a temperature of 350°C is chosen for subsequent testing of the NiTi specimens so as to provide the smallest strains after a large number of cycles.

The results showed that the maximum equivalent viscous damping values occurred between the 4% strain cycle and the first 6% strain cycle. The equivalent viscous damping values increased with increasing annealing temperature. Although damping is desired for seismic rehabilitation, past studies have shown that the recentering capability is more important for restrainer cable applications in bridges. The maximum equivalent viscous damping values at the first 6% strain cycle for the 500°C annealed NiTiCr specimen and 450°C annealed NiTi specimen were approximately 4.6% and 5.6%, respectively, as compared to those annealed at the temperature determined ideal based on recentering capability which resulted in a decrease in equivalent viscous damping to values of 2.9% and 3.0% for the NiTiCr and NiTi specimens at the first 6% strain cycle, respectively.

Comparing the cyclic behavior of the NiTiCr specimens annealed at 450°C to the cyclic behavior of the NiTi specimens annealed at 350°C, it can be seen that both the ternary and binary specimens provide good superelastic behavior when cycled quasi-statically. Both types of SMAs provide similar damping capabilities at these temperatures, but the NiTiCr specimen has slightly better recentering capabilities. This suggests the possibility of using other ternary shape memory alloys for seismic applications.

Strain Rate Study

After determining the annealing temperature that is optimal for seismic applications of both NiTiCr and NiTi SMAs in bridges, the two types of specimens were subjected to a strain rate study to determine if their cyclic properties are affected by strain rates associated with those experienced in bridge systems during an earthquake. Uncycled specimens annealed at the temperatures determined during the annealing testing underwent a far field type loading protocol at strain rates of 0.025 Hz, 0.5 Hz, 1.0 Hz, and 2.0 Hz. Although 350°C provided the least residual strain for the NiTi specimens, an annealing temperature of 400°C was used to anneal the NiTi specimens during this study to provide some added damping. Future tests will be conducted with an annealing temperature of 350°C for the NiTi specimens. Two specimens of both the ternary and binary SMAs were used at each strain rate to ensure repeatability of the results. Figure 11 provides the stress-strain curve for the NiTiCr wire specimens cycled at 0.025 Hz and 1.0 Hz. The results for the NiTi wire specimens cycled at the same strain rates can be found in Figure 12. It is obvious from the two figures that the cyclic properties of NiTi based shape memory alloys are affected by an increased strain rate. For both the

NiTiCr and NiTi, the hysteresis decreases with an increased loading rate due to a significant increase in the reverse transformation stress (martensite to austenite) and a slight decrease in the forward transformation stress (austenite to martensite).

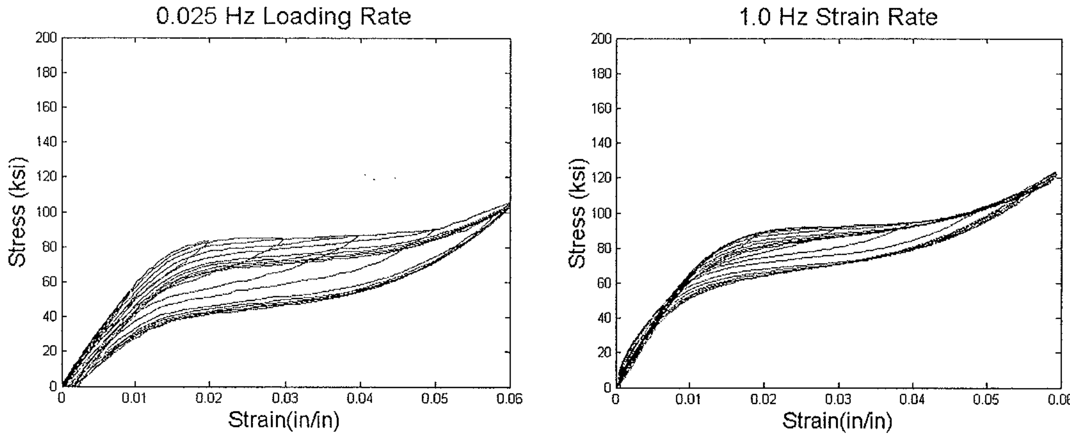

Figure 11. Stress-Strain Curves for NiTiCr at Loading Rates of 0.025 Hz and 1.0 Hz

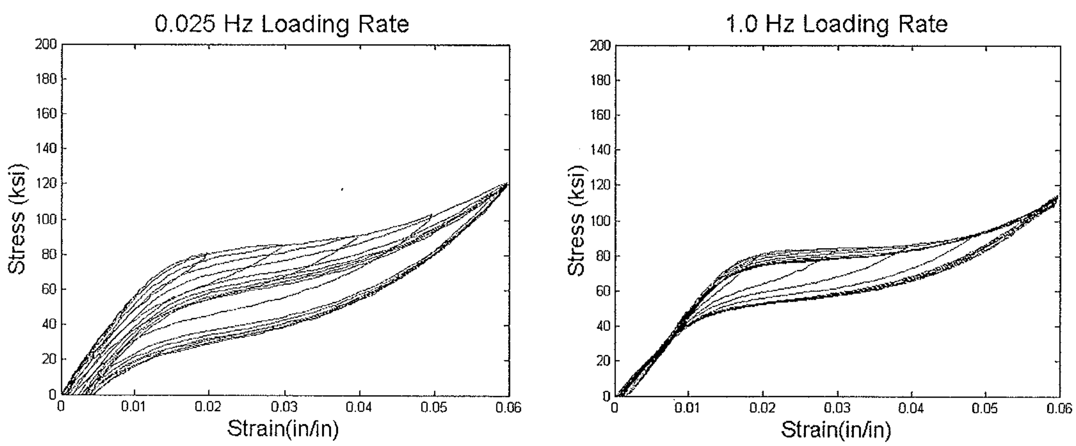

Figure 12. Stress-Strain Curves for NiTi at Loading Rates of 0.025 Hz and 1.0 Hz

Due to the pinching of the hysteresis, the equivalent viscous damping value decreases with the increased strain rate. The equivalent viscous damping value at the first 6% strain cycles decreases from approximately 2.9% when cycled at 0.025 Hz to 1.5% when cycled at 1.0 Hz for the NiTiCr specimen and decreases from approximately 3.0% when cycled at 0.025 Hz to 2.2% when cycled at 1.0 Hz for the NiTi specimen. The NiTiCr specimen has a larger drop in equivalent viscous damping as compared to that experienced by the NiTi specimen. Although the equivalent viscous damping value decreases with increased strain rate, it is apparent from the results that the residual strain decreases providing an increase in the recentering capability with increased strain rate. The NiTiCr specimen has a maximum residual strain of approximately 0.2% and 0.062% when cycled at strain rates of 0.025 Hz and 1.0 Hz, respectively. The maximum residual strain for the NiTi specimen also decreases with increased strain rate from 0.4% to 0.12% for the 0.025 Hz and 1.0 Hz rates, respectively. **The results of the materials tests show the viability of using both NiTiCr and NiTi as a recentering device in bridges.**

Traditional Unseating Prevention Devices

Since the 1971 San Fernando earthquake, which resulted in the collapse of more than 60 bridges, a significant number of research studies had been conducted to better understand the problem of unseating in bridges during earthquakes (Cooper and Friedland 1994). Figure 13 shows the unseating of several spans of the Route 210/5 Interchange during the 1971 San Fernando earthquake. After the earthquake, the California department of transportation (Caltrans) initiated a state-wide seismic retrofit program to systematically retrofit older and non-ductile bridges. Cables and rods that were made of steel were used to limit relative hinge displacement between spans and reduce the likelihood of unseating. Although the restrainers performed adequately during the 1989 Loma Prieta and the 1994 Northridge earthquakes, there were several instances of failure of the cables and/or connecting elements. The design procedures for the steel restrainers require the restrainers to remain elastic during earthquakes, which causes either the restrainers to break or the diaphragm walls at the two ends of the cable restrainer to suffer punch-through action during a severe earthquake (Feng et al. 2000). Since the restrainers are designed to remain elastic, they lack the ability to dissipate energy, which is a major drawback during earthquakes. The collapse of the Gavin Canyon Undercrossing and the 14/5 Interchange during the 1994 Northridge earthquake has proven the inadequacy of the currently used steel restrainers (Saiidi et al. 2001).

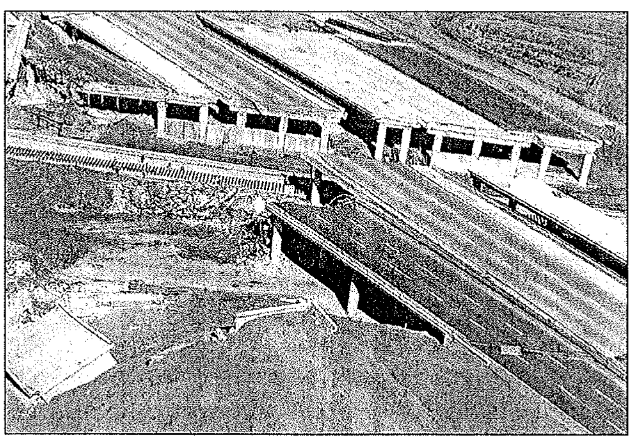

Figure 13. Unseated spans in the 210/5 Interchange during the 1971 San Fernando earthquake (NISEE Collection)

A number of other devices were presented in the past two decades as unseating prevention devices in bridges such as the fluid viscous dampers, which are a velocity-dependant type of dampers (HITEC Report 1999), and the metallic dampers, which are considered as force-dependant dampers (Chen et al. 2001). Although these devices are energy dissipation devices, they lack the capability to recenter, which is important to control the hinge opening in bridges. The SMA restrainers in its superelastic phase are characterized by a large elastic strain (6%-8%), which means that the SMA restrainers are capable of recovering its original length even under severe earthquakes. Therefore, SMAs, which have both damping and recentering, offer a unique set of capabilities not seen in current devices. Another advantage of using these devices is the fact that the shape of the SMA hysteresis is controlled by the manufacturing procedures used in developing the alloy, thus a yield-like hysteretic plateau could be developed for the SMA restrainers, limiting the force transferred to adjacent frames. Also, once the SMA restrainers are deformed beyond its elastic range, it strain hardens. This behavior induces high level of force, which is required to prevent unseating in the case of strong ground motions.

Analytical Study to Evaluate the Effectiveness of Superelastic NiTi SMA Restrainers

The traditional steel cable restrainers and rods used have several limitations, including small elastic strain range, and limited ductility capacity. To address some of the limitations of current unseating prevention devices, a new technology, using Nitinol SMAs is proposed as unseating prevention devices. Superelastic SMAs have the ability to remain elastic under very large deformations, due to a solid-state martensitic transformation. This unique property leads to enhanced performance of the adaptive superelastic unseating prevention device, compared with conventional devices used in the United States and Japan. The study presented evaluates the effectiveness of these devices in limiting relative hinge displacements in typical multiple frame bridges. To assess the effectiveness of the devices, nonlinear time history analyses are performed on a typical multiple frame reinforced concrete box girder bridge using a suite of representative ground motions.

Analytical Models

Bridge as-built model

A multiple frame bridge identical to the type of bridge typically constructed in California was considered in the analysis. Figure 14 shows the elevation of the analyzed bridge. As shown in the figure, the bridge consists of two interior taller frames (Frames 2 and 3) and two exterior shorter frames (Frames 1 and 4). The interior frames have a total length of 183 m (600') and a total height of 18 m (60'). The exterior frames have a total length of 73 m (240') and a total height of 12.2 m (40'). The bridge's superstructure consists of a concrete box girder supported on concrete piers. The nonlinear dynamic program DRAIN-2DX was used in analyzing the bridge (Prakash 1992). The plastic hinge beam-column element (Type 02) was used in modeling the bridge's superstructure and columns. This element consists mainly of an elastic element joining two plastic hinges. The Type 02 element takes into account the inelastic behavior of the element through the formation of plastic hinges at the two end nodes of the element. Under earthquake loadings, the bridge deck is expected to behave elastically. Hence, the superstructure of the bridge was modeled to remain elastic, while two values of yield strength were used in modeling the columns based on its flexibility. The bent caps were modeled using a rigid element connecting the girders with the columns. The nonlinear behavior of the abutments was modeled in Drain-2DX using Type 09 link elements. The Type 09 link element is an inelastic bar which resists only uniaxial loads. The element is used as either tension-only or compression-only with an initial slack or gap. Two link elements with elastic perfectly plastic behaviors were used in parallel to model the active and passive resistance of each abutment. A compression-only link element was also used to model the impact effect between the bridge components. A 50.8-mm (2 in.) gap and a 12.7 mm (0.5 in.) gap were assumed at the exterior and interior hinges of the bridge, respectively.

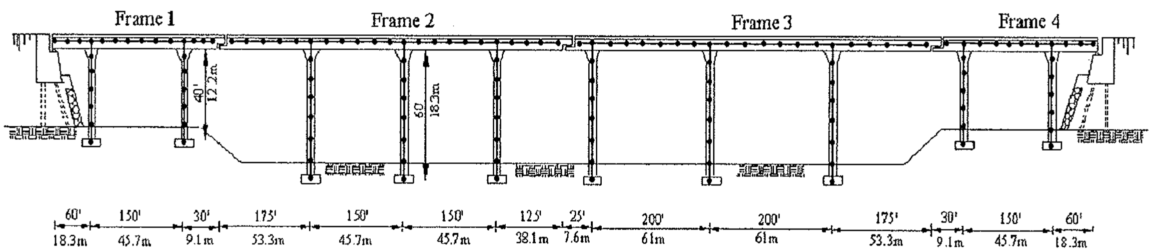

Figure 14. Four-frame box girder bridge considered in the analysis

Restrainer modeling

Two types of restrainers were involved in the analysis: the regular steel cable restrainers and the superelastic SMA restrainers. The steel restrainers are modeled as a bilinear element. Once the element yields it unloads inelastically developing a residual strain. The element was modeled to represent the actual behavior of steel restrainers, which accumulates residual strain upon successive yielding. On the other hand, the constitutive behavior of the superelastic SMA restrainer was modeled through the parallel combination of two Type-09 link elements and a Type-01 truss element, which is a tension-compression bilinear element. However, in this study it was used as tension-only element. Figure 15 shows a schematic of the model that was developed to describe the superelastic behavior in SMAs. As shown in the figure, the initial branch and the strain hardening branch were modeled using the two link elements, while the truss element was utilized in developing the hysteretic behavior of the SMAs. The stiffness of the SMA model was calculated form the superposition of the three elements stiffness. In this study, the steel and superelastic restrainers were modeled as with a 12.7-mm (0.5 in) slack.

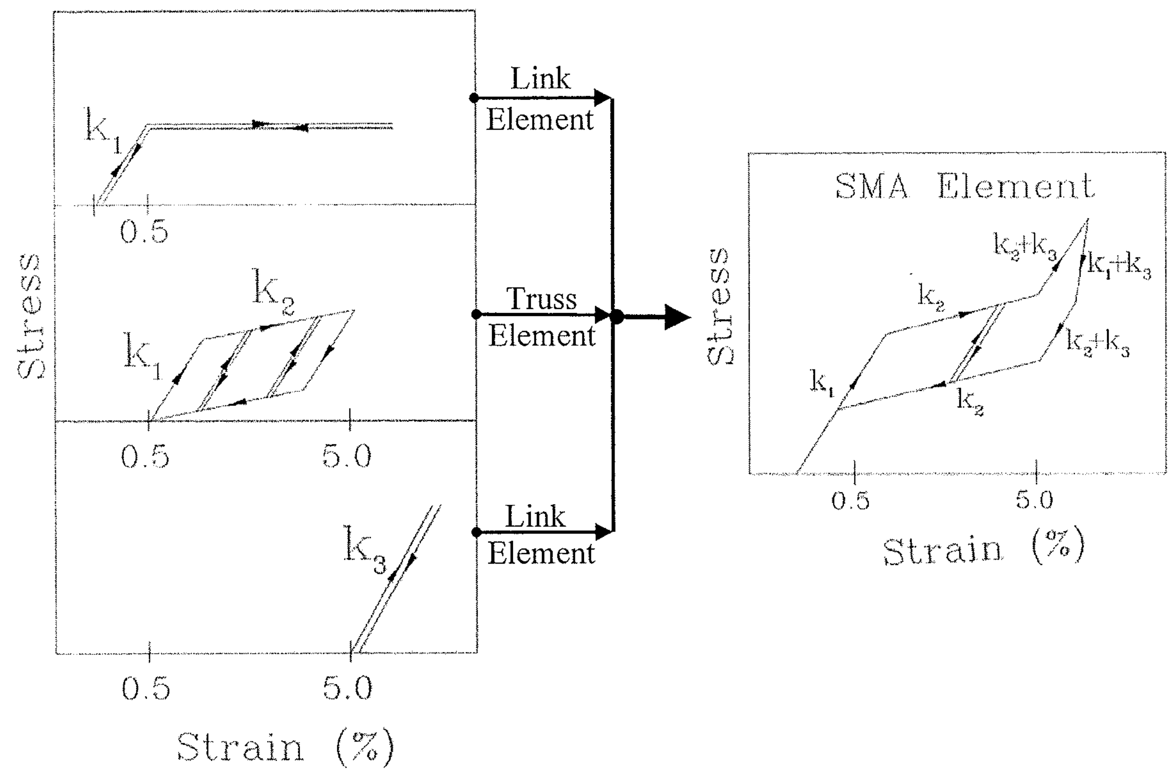

Figure 15. Schematic of the superelastic SMA model developed using 2 link elements and a truss element in Drain-2DX.

Design of Restrainers

Steel restrainer design

Steel restrainers were designed using the AASHTO restrainer design procedure (AASHTO 1992). In this method, the designer calculates the force resisted by the restrainers through multiplying the mass of the lighter frame with a certain acceleration value. In this study, a 3.05 m (10 ft) length steel cable was used based on a target hinge displacement equal to 63.5mm (2.5in). The length of the restrainers was selected such that it would remain elastic under a target hinge displacement of approximately 63 mm (2.5 in). A value of 0.7g peak ground acceleration was assumed and used to calculate the force required to restrain each frame. The force required between the outer and inner frames was 16800 KN (3777 kips), while the force required between the two internal frames was 37300 KN (8393 kips). The required forces result in approximately 100 restrainers at each of the exterior hinges and 215 restrainers at the interior hinge. These numbers were considered to be extremely large compared to the actual number of restrainers used in bridges. Since the preliminary modal analysis of the bridge indicated that the two interior frames would vibrate in-phase while the exterior and interior frames would vibrate out-of-phase, more restrainers were required at the exterior hinges compared to the interior hinge. This showed that applying the AASHTO design procedure is not appropriate in this study since it depends mainly on the weight of the frames rather than their period ratios. Instead, a practical number of 25 restrainers were used in all of the three hinges. This number is a typical number for the restrainers used by Caltrans in multiple frame bridges. In order to be conservative in this study, the same number of restrainers was used in each of the three hinges.

Superelastic restrainer design

The superlelastic rods used in the analysis were 12.7 mm (0.5 in) in diameter, 914 mm (36 in) in length. The rods were designed to have a maximum force equal to that in the 25 steel restrainers. The stress-strain curve resulting from the quasi-static test conducted by Delemont (2002) in Phase I of this project was used in the analysis. Figure 16 shows the superelastic stress-strain curve that was used in the analysis. A value of 5% was assumed for the elastic strain range. The SMA restrainers were designed such that they would reach the same level of force as the steel restrainers at the same elastic strain. At 5% strain in the superelastic restrainers, the force was found to be approximately, 3737 KN (840 kips). Fifty five SMA restrainers were found to be sufficient to produce such force at the 5% strain level.

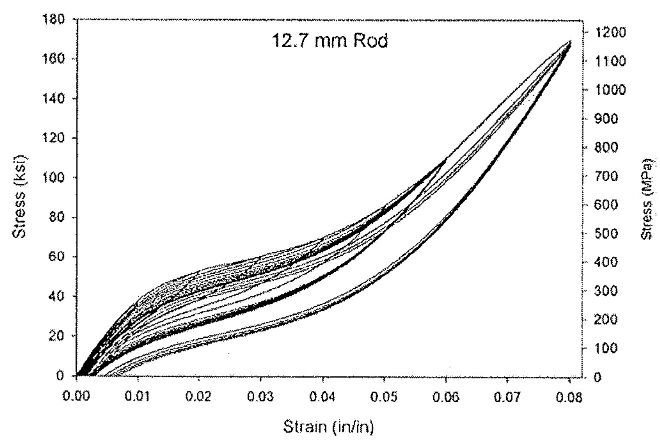

Figure 16. Typical stress-strain curve of the 12.7-mm diameter Nitinol superelastic rods considered in the analysis (Delemont, 2002 – Phase I)

Ground Motions

A suite of 10 ground motion records consisting mainly of historical earthquakes that occurred in California in the past 25 years was used in this study. The records were selected to cover a range of ground motion characteristics such as the peak ground acceleration, duration, and frequency content. Table 2 shows a description and characteristics of the ground motions (magnitude, epicentral distance, duration, peak ground acceleration, and predominate period) used in the analysis. Since this study is focusing on the performance of typical California multiple frame bridges, each ground motion record was scaled to a value equal to the design spectral acceleration value of the San Francisco area at the predominate period of the structure (1.67 sec). The last column in Table 1 shows the spectral acceleration value (S_{an}) for each record at the natural period of the studied bridge. Using the 10% probability of exceedence in 50 years USGS seismic hazard maps with site class B, the code-based design response spectrum was developed. Figure 17 shows a comparison between the code-based design response spectrum and the average response spectrum of the 10 ground motion records after they were scaled. As shown in the figure, both spectra intersect at a value of 0.28g at the predominate period of the structure. Note, however, for shorter periods, the mean response spectrum of the 10 ground motions used in the analysis far exceeds the code-based design spectrum.

Record description	Earthquake magnitude (M_w)	Distance (km)	Duration (sec)	PGA (g)	Tg (sec)	S_{an} (g)
1994 Northridge, Beverly Hills	6.7	20.8	23.9	0.62	0.26	0.18
1986 N. Palm Springs, North Palm Springs	6.0	8.20	20.0	0.69	0.34	0.12
1979 Imperial Valley, SAHOP Casa Flores	6.5	11.1	15.7	0.51	0.42	0.18
1989 Loma Prieta, Gilroy Array #3	6.9	14.4	39.9	0.56	0.47	0.13
1992 Cape Mendocino, Rio Dell Overpass	7.1	18.5	36.0	0.55	0.48	0.14
1983 Coalinga, Pleasant Valley	5.8	17.4	21.7	0.60	0.69	0.11
1983 Coalinga, Transmitter Hill	5.8	9.20	21.7	0.84	0.72	0.16
1994 Northridge, Tarzana, Cedar Hill	6.7	17.5	40.0	0.99	0.74	0.32
1992 Cape Mendocino, Petrolia	7.1	9.50	36.0	0.66	0.76	0.44
1989 Loma Prieta, WAHO	6.9	16.9	24.9	0.64	0.98	0.17

Table 2. The suite of ground motion records selected for the analysis

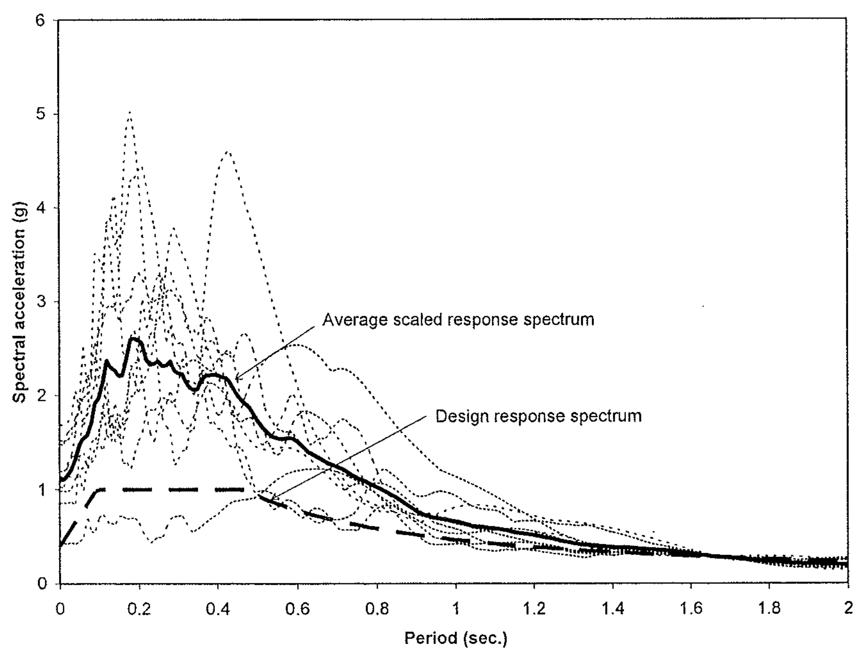

Figure 17. The design response spectrum (dashed) used in the analysis compared to the scaled response spectra of the ground motions suite

Analysis Results

Figure 18 shows the maximum hinge openings resulting from the analysis of the multiple frame bridge under the suite of ground motions. For each record the analysis was performed without restrainers (as-built), with steel cable restrainers (steel) and with superelastic SMA restrainers (SE). As shown in the figure, the degree of effectiveness of each of the two restrainer types varied from one record to another. However, in all cases the SE restrainers were more effective in reducing the maximum hinge opening.

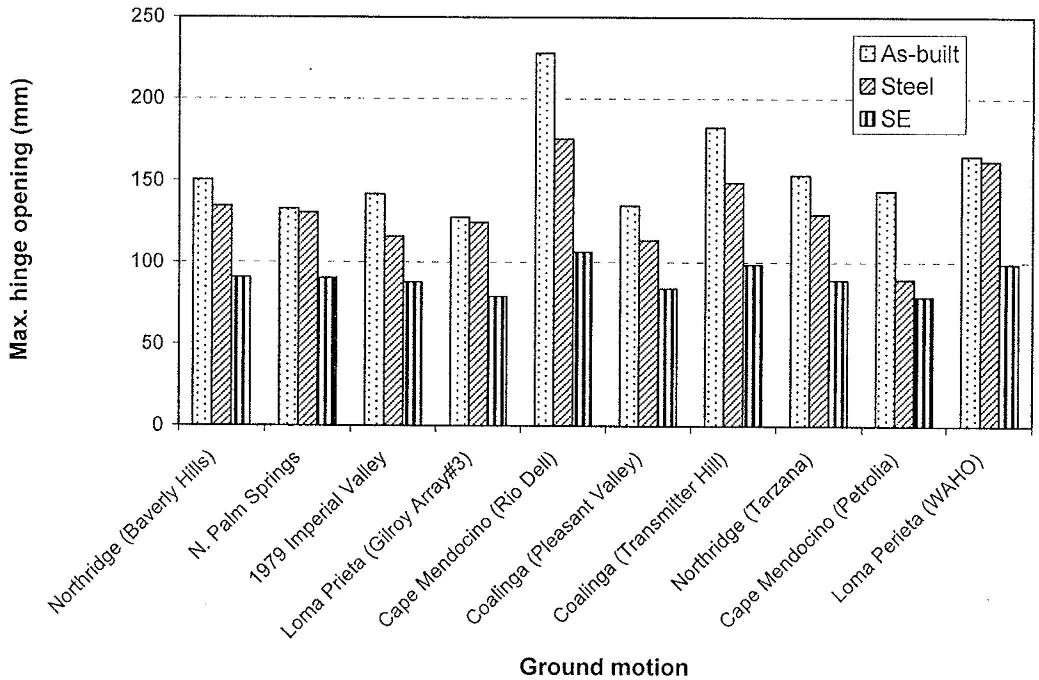

Figure 18. Maximum hinge opening for various ground motions

The maximum effectiveness of steel restrainers was observed in the case of the 1992 Cape Mendocino (Petrolia) ground motion, where the maximum hinge opening was reduced by approximately 37% compared to the as-built case. Three cases showed a poor performance for the steel restrainers, where the restrainers experienced a significant amount of yielding, which reduces the effectiveness of the restrainers and results in a small reduction in the maximum hinge opening [1986 North Palm Springs, the 1989 Loma Prieta (Gilroy Array #3), and the 1989 Loma Prieta (WAHO)]. However, the SE restrainers produced a significant amount of reduction in the maximum hinge openings that varied between 31% and 62% approximately. The average amount of reduction resulting from using the SE restrainers was 43%, while the reduction for the steel cable restrainers was approximately 16%.

Figure 19 shows the residual hinge opening resulting at the end of each record for both types of restrainers in addition to the as-built case. The SE restrainers were effective in reducing the residual hinge opening in most cases, particularly for the cases where the bridge frames experienced large residual hinge opening in the case of no restrainers (as-built). However, in the cases were the residual hinge openings in the as-built bridge were relatively small such as in the cases of Coalinga (Pleasant Valley) and Northridge (Tarzana) records the SE restrainers slightly increased the residual hinge openings. This increase is most likely due to the large level of force reached during the strain hardening of the SE restrainers. This large force plays an important role in limiting the maximum hinge openings in the case of strong earthquakes were unseating is expected. However, in the case of moderate earthquakes the level of force is significantly reduced resulting in a reduction in the residual hinge openings. Figure 9 also shows that the 1979 Imperial valley record did not produce a residual displacement in the hinge. It is also shown that in the cases of the Northridge earthquake (Beverly Hills), the North Palm Springs earthquake (North Palm Springs) and the Loma Prieta earthquake (WAHO) records, the steel restrainers increased the residual hinge openings compared to the as-built case. This behavior is due to the lack of recentering that is asscociated with the steel cable restrainers' type.

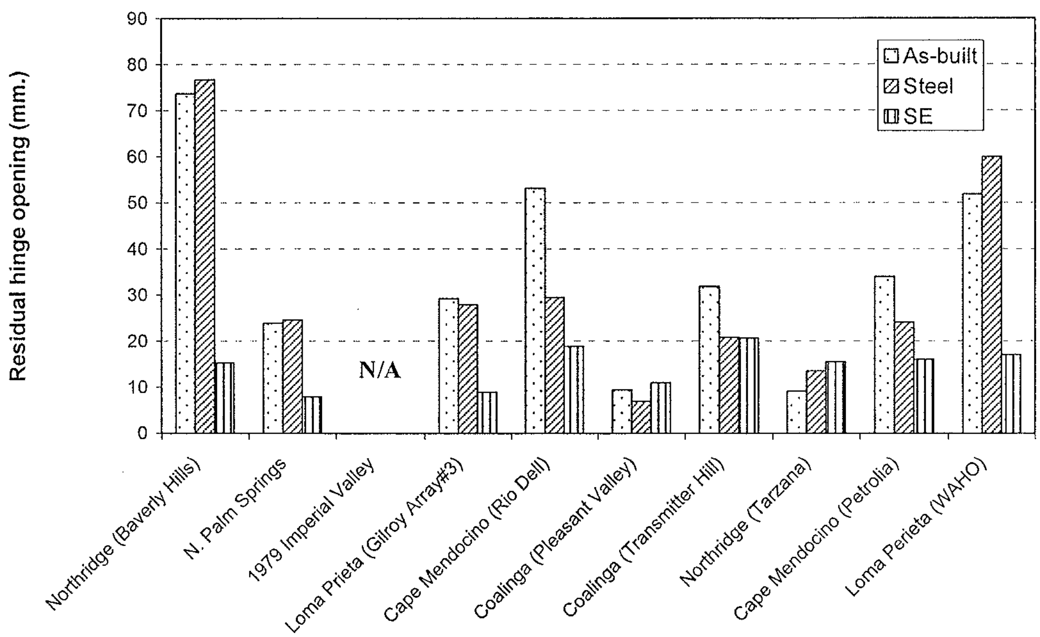

Figure 19. Residual hinge openings for various ground motions

Previous studies have shown that one of the drawbacks of using restrainers is that they tie separate spans together, which can increase the force transferred between the two connected frames and thereby increase its lateral drifts. Figure 20 shows a comparison between the maximum frame drifts resulting from each record for the SE restrainers' case, steel cable restrainers' case and the as-built case. The figure shows that the effect of restrainers on the drifts in the frames is minor. In most of the cases the existence of the restrainers slightly increases the frame drifts. However, for the majority of the cases the frame drifts produced in the case of the SE restrainers is smaller than that produced in the case of steel restrainers.

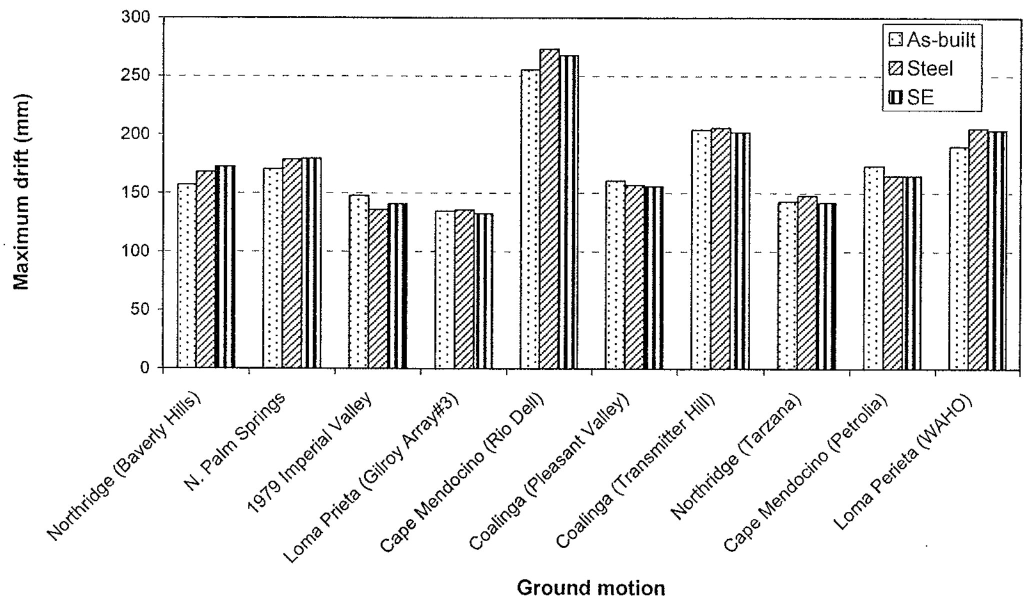

Figure 20. Maximum frame drift for various ground motions

To better understand the effectiveness of SE restrainers versus steel restrainers, the time history response of the 1989 Loma Prieta (Gilroy Array #3) is presented in this section. Figure 21 shows the time history of the relative hinge opening at the hinge between frames 3 and 4. As shown in the figure, the SE restrainers were effective through the entire record and reduced the maximum hinge opening by approximately 38% compared to the as-built case. However, the steel restrainers showed an effective performance in the first cycle (before yielding). Points A and B show the maximum response for steel restrainers and SE restrainers, respectively during the first major cycle before yielding. The responses of the steel and SE restrainers were similar. However, once the steel restrainers yielded, they began accumulating residual strains and their effectiveness was reduced significantly. This behavior is demonstrated through points C and D on the figure. Point C represents the maximum response in the case of steel restrainers during the seventh major cycle, while point D represents the maximum response in the case of SE restrainers at the same cycle. The difference in the performance between the SE and steel restrainers increased significantly in the seventh cycle compared to the first cycle. This is due to the fact that the steel restrainers accumulate strain once it experiences yielding, thus reducing its effectiveness. The maximum hinge opening in the steel restrainers' case was approximately equal to that in the as-built case.

Figure 22 shows the force-displacement relationship for the two types of restrainers. Points A, B, C, and D that were previously discussed in Fig. 21 are shown in the figure. The response at points A and B were close since the steel restrainers were acting in its elastic stage. Once the steel restrainers experience yielding (point C) it loses its efficiency. The figure also illustrates that the recentering behavior of the SE restrainers played an important role in controlling the hinge opening. The strain hardening of the SE restrainers assists in minimizing the possibilities of frame unseating in the case of strong ground motions.

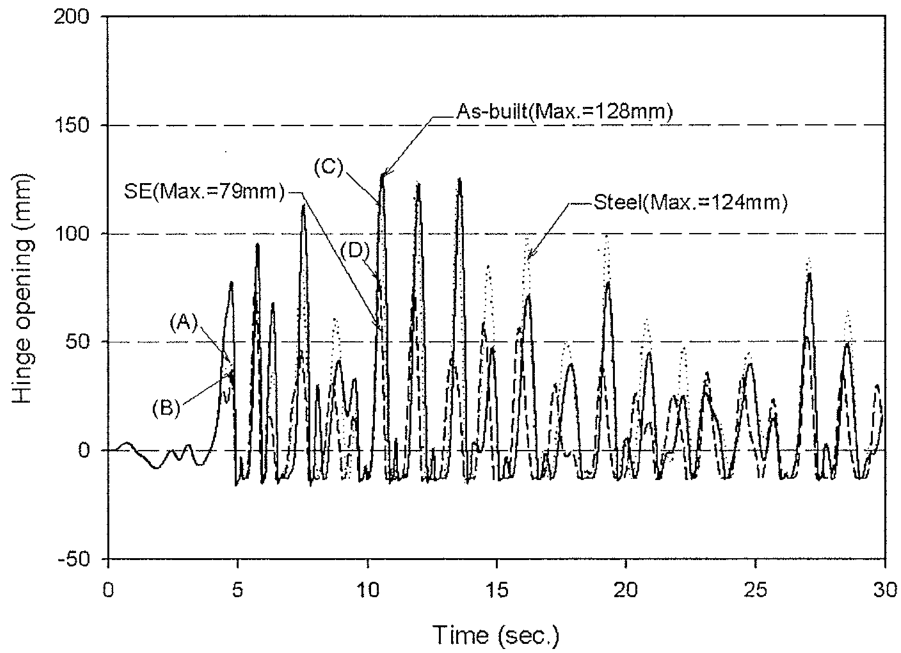

Figure 21. Hinge opening time history for the Loma Prieta, (Gilroy Array #3) ground motion record

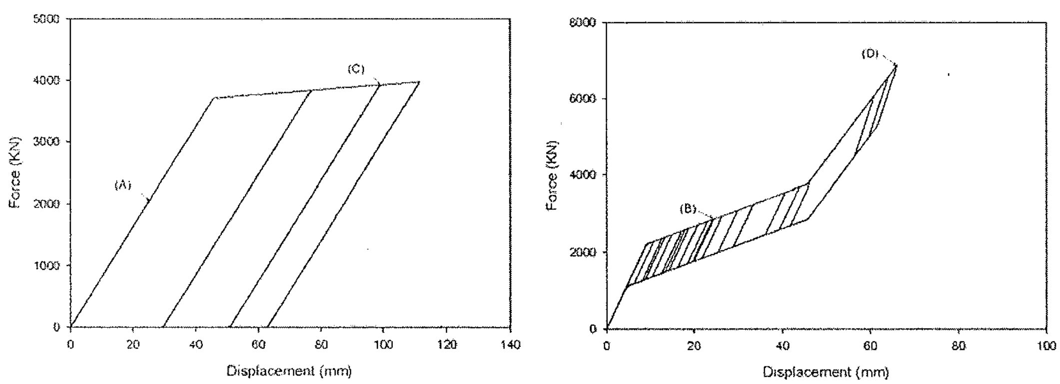

(a) Steel restrainers **(b) SE restrainers**

Figure 22. Force-displacement relationship for the steel restrainers and SE restrainers under the Loma Prieta (Gilroy Array #3) ground motion record

Figure 23 shows the time history of the drift in frame 3. Similar behavior is observed in the three cases (as-built, steel, and SE). This shows that although the SE restrainers transfer larger force to the connected frames compared with the steel cable restrainers, the maximum frame drifts were not affected by this force due to the recentering capability of the SE restrainers. This shows that using the SE restrainer does not increase the ductility demand on the bridge frames.

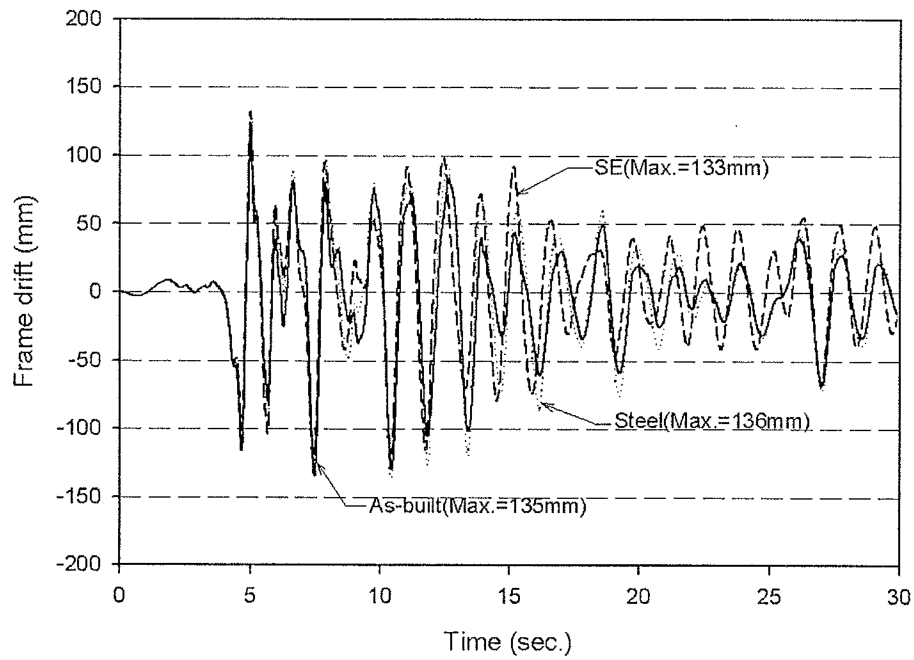

Figure 23. Drift time history of frame (3) for the Loma Prieta (Gilroy Array #3) ground motion record

Conclusions from Analytical Study of Nitinol SMA Restrainers

A study was conducted to evaluate the efficacy of superelastic Nitinol shape memory alloy restrainers in preventing the unseating of multiple frame bridges during strong ground motions. A nonlinear dynamic analysis was conducted using a suite of 10 ground motion records. The performance of a typical California multiple frame reinforced concrete box girder bridge was evaluated using the superelastic restrainers and the traditional steel cable restrainers.

The superelastic elements reduced the relative hinge displacements significantly compared to the steel restrainers. The high elastic strain of the superelastic elements in addition to its damping characteristics were the primary factors behind its effectiveness. The steel restrainer performed poorly in most of the cases due to its low elastic strain limit. The maximum hinge opening for the SE restrainers' case, the steel cable restrainers' case, and the as-built case were compared and analyzed. The response time history showed that during the first few cycles both types of restrainers perform similarly. Once the steel restrainers yield it begins accumulating residual strain and thus its effectiveness is reduced significantly. However, the SMA superelastic restrainers remain effective during the entire time history due to its capability to recenter and recovering its original length after being deformed to a level of strain that can reach 6%-8%.

The analysis of the frame drifts of the multiple frame bridge using the SMA restrainers, and the steel cable restrainers showed that the type of restrainer has a minor effect on the maximum drifts of the bridge frames. Although the SMA restrainers transfer more force to the connected structural elements, the ductility demand on the frames was not affected. **This study showed that the superelastic elements are capable of reducing the relative hinge displacements in multiple frame bridges during strong ground motions without increasing the ductility demand on the bridge frames and thus preventing the unseating of the bridge superstructure.**

Preliminary Analysis & Development of Testing Setup For ¼ Scale Tests of SMA Restrainer in Multiple Frame Bridge

In the stage of the project, concepts for the application of Shape Memory Alloys for bridge structures is evaluated. First, Preliminary analysis is performed to determine the design parameters for the test setup. Next, a testing setup is developed, using a ¼ scale shape table facility at the University of Nevada, Reno.

Preliminary Analysis for SMA Restrainer Tests

Based on the configuration of the shake table, and expected input, the following parameters shown in Table 3 were considered in the design of the experiment.

	Case 1	Case 2
Mass of Block 1 (M_1) k-s^2/in (kN-s^2/m)	0.76 (133)	0.76 (133)
Mass of Block 2 (M_2) k-s^2/in (kN-s^2/m)	0.53 (92.9)	0.53 (92.9)
Stiffness of Block 1 (K_1) k/in (kN/m)	2 (31.0)	2 (31.0)
Stiffness of Block 2 (K_2) k/in (kN/m)	4 (62.0)	4 (62.0)
Number of Restrainers	3 (52.5)	5 (87.5)
Size of Restrainers (diameter) in (mm)	1/8" (3.18)	1/8" (3.18)
Restrainer Stiffness (K_r) k/in (kN/m)	2.43 (425)	4.04 (708)
Restrainer Length in (m)	158 (4)	158 (4)
Restrainer Stiffness Ratio(K_r/K_1)	1.2	2.0
Slack (s) in (mm)	0.0 (0)	0.50 (12.7)
Gap (g) in (mm)	0.40 (10.2)	0.40 (10.2)
Ground Motion Peak PGA	Case 2 (0.20g)	Case 3 (0.30g)

Table 3. Test Parameters

For the test using SMA, both the *effective* restrainer stiffness and the force in the cable are set equal to each other. The effective restrainer stiffness for the steel cable is based on the yield strain of approximately 1.5%, which the effective SMA restrainer stiffness is based on the secant stiffness at 6% strain (See Figure 24).

$K_r = E_rA_r/L_r$ (eq 1a)
$K_{sma} = E_sA_{sma}/L_{sma}$ (eq 1b)

$F_{yr} = A_r\sigma_{yr}$ (eq 2a)
$F_{sma} = A_{smay}\sigma_{sma}$ (eq 2b)

Where,

K_r is the steel restrainer effective stiffness
K_{sma} = effective stiffness of SMA restrainers
E_r= steel modulus of elasticity steel restrainers
E_{sma} = modulus of elasticity of SMA restrainers
A_r=area of steel restrainers
A_{sma} = area of SMA restrainers
L_r = Length of steel restrainers
L_{sma} = length of SMA restrainers
F_r = yield force in steel restrainers
σ_{yr} = yield stress on steel restrainers
F_{sma} = yield force in steel restrainers
σ_{ysma} = yield stress on steel restrainers
Setting F_{yr} = Fsma and $K_r=K_{sma}$

$A_s = A_rF_{yr}/F_{sma}$ (equ 3) $L_{sma} = L_r*E_{sma}/E_r*F_{yr}/F_{sma}$
(equ 4)

The table below shows the resulting design for the SMA restrainer cable for case 1 and case 2. The following parameters are fixed

Er = 21,300 ksi
Esma = 1,466 ksi (based on 6% strain)
Lr = 158 inches
σ_{ysma} = 80 ksi
σ_{yr} = 350 ksi

$A_s = A_rF_{yr}/F_{sma}$ (equ 3)
$(0.018\ in^2)*(311\ ksi)/(80\ ksi)$
$=0.070\ in^2$

Diameter of SMA Required
$\pi/4*d^2=A_s=0.070\ in^2$

(Case 1: 1 bar @ d=0.30 in) or (Case 2: 1 bar @ d=0.50 in)
(Case 1: 2 bars @ d= 0.21 in) or (Case 2: 2 bars @ d= 0.28 in)

	Case 1	Case 2
STEEL RESTRAINER CABLES		
Number of Restrainers	3	5
Size of Restrainers (diameter)	1/8" (3.18)	1/8" (3.18)
Area of Restrainers in^2 (mm^2)	0.018 (11.6)	0.03 (19.3)
Restrainer Stiffness (K_r) k/in (kN/m)	2.43 (423)	4.04 (707)
Restrainer Length in (m)	158 (4)	158 (4)
SMA RESTRAINER CABLES		
Number of SMA Restrainers	2	2
Diameter of SMA Restrainers (bar)	0.30 in (7.62 mm)	0.50 in (12.7 mm)
Size of SMA Restrainers (wire)	84x0.023"	130x0.023"
Area of SMA Restrainers	0.07 in^2 (45.6)	0.1166 in^2 (74.8)
SMA Restrainer Stiffness k/in (kN/m)	2.427 (423)	4.04 (707)
SMA Restrainer Length in (m)	42" (1.07)	42" (1.07)

Table 4: Summary of Steel and SMA Restrainer Cables

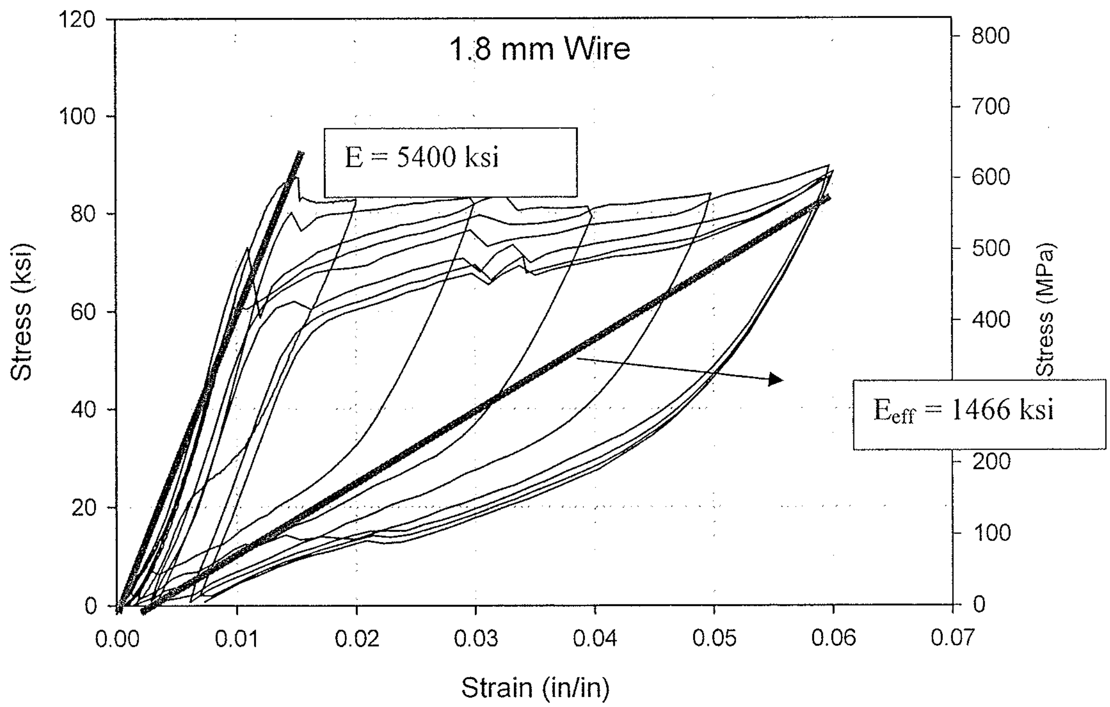

Figure 24. Stress-Strain Plot of SMA wire showing effective stiffness at 6% strain

Preliminary Analysis Results

Preliminary analysis is performed to compare the performance of the SMA restrainer with the SMA restrainers using the parameters and ground motion given by UNR. The model is a simple 2-DOF with mass and stiffness from the blocks as seen in Figure 25. The nonlinear tension only behavior of the restrainers and the nonlinear compression-only behavior of impact is represented. Friction was not included in the model, since it is not clear what friction force is used.

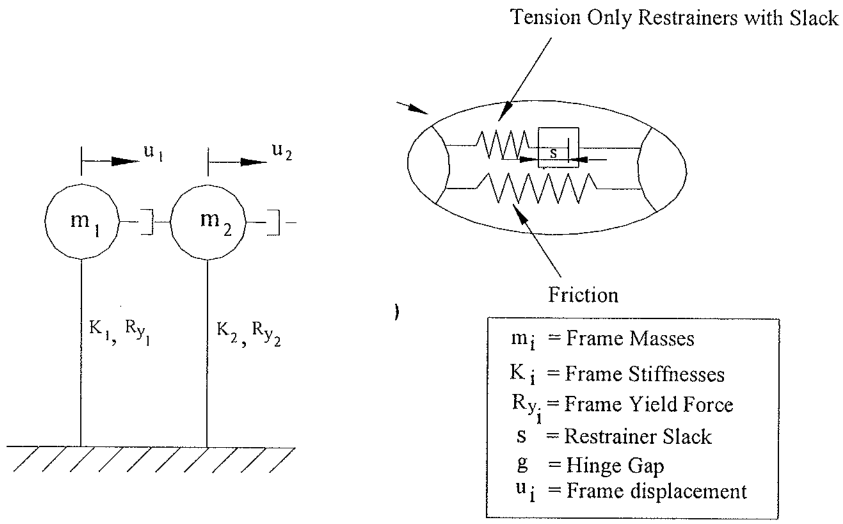

Figure 25. Analytical model of test set-up for design and preliminary studies

The results of the analysis are shown below for Case I in which there is a restrainer stiffness ratio of 1.2 (3-1/8" cables), zero slack, and a PGA of 0.2g. Figure 26 displays the time history of the relative hinge opening for the test set-up with no restrainer, steel restrainers, and SMA restrainers. The anticipated force displacement relationship for the steel restrainer cable and SMA restraining device is shown in Figure 27.

The results of the analysis are also displayed below for Case II. In this case there is a restrainer stiffness ratio of 2.0 (5 - 1/8" cables), 0.5 in slack, and a PGA of 0.3g. Figure 28 displays the time history of the relative hinge opening for the Case II test set-up with no restrainer, steel restrainers, and SMA restrainers. Figure 29 shows the anticipated force displacement relationship for the steel restrainer cable and SMA restraining device.

Table 5 presents a summary of the results of the preliminary study of the test set-up for ¼ scale tests of SMA restrainers in a multiple frame bridge. These results indicate an anticipated maximum hinge opening and maximum cable force for two different test set-ups. The results of this study were used to develop and verify the experimental test set-up to be utilized in a test at University of Nevada, Reno Large Structures Laboratory, in cooperation with investigators at the University of Nevada, Reno.

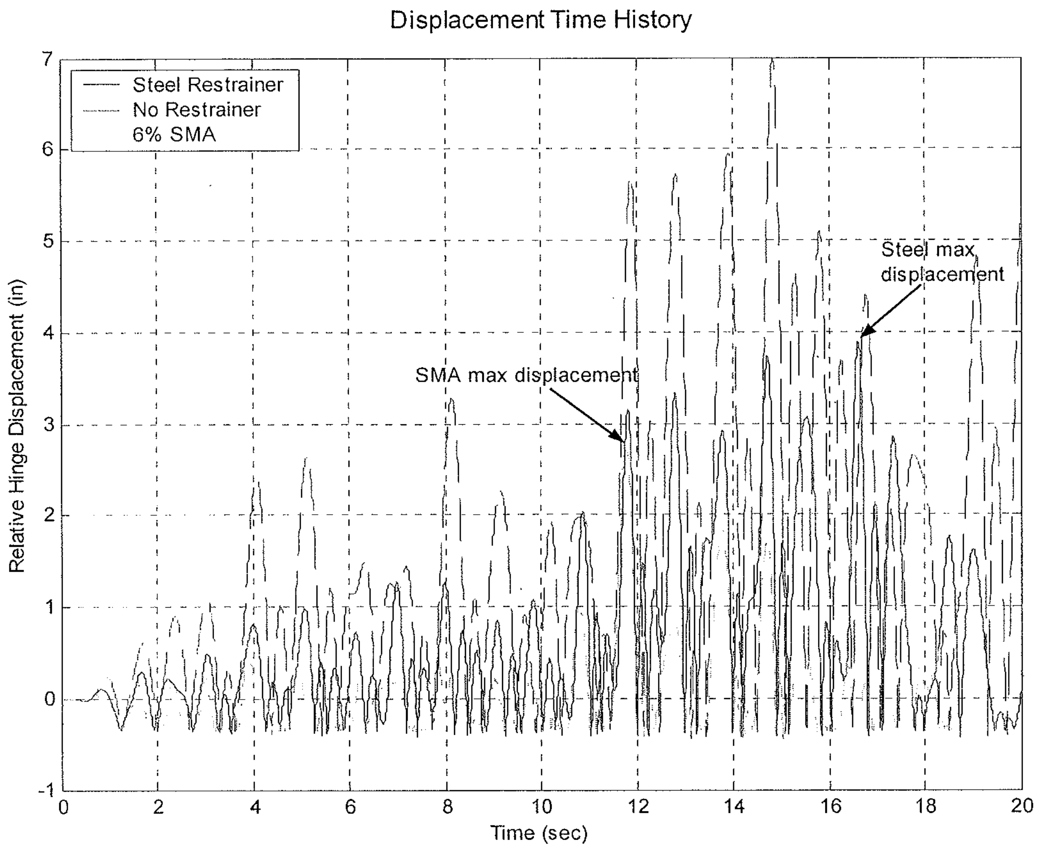

Figure 26. Analytical results for time history of relative hinge displacement (Case I)

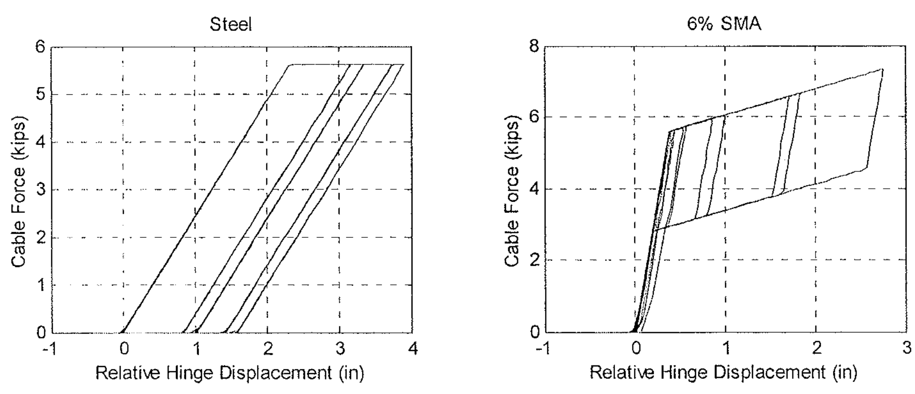

Figure 27. Analytical results for force-displacement of steel cable restrainers and SMA cable restrainers (Case I)

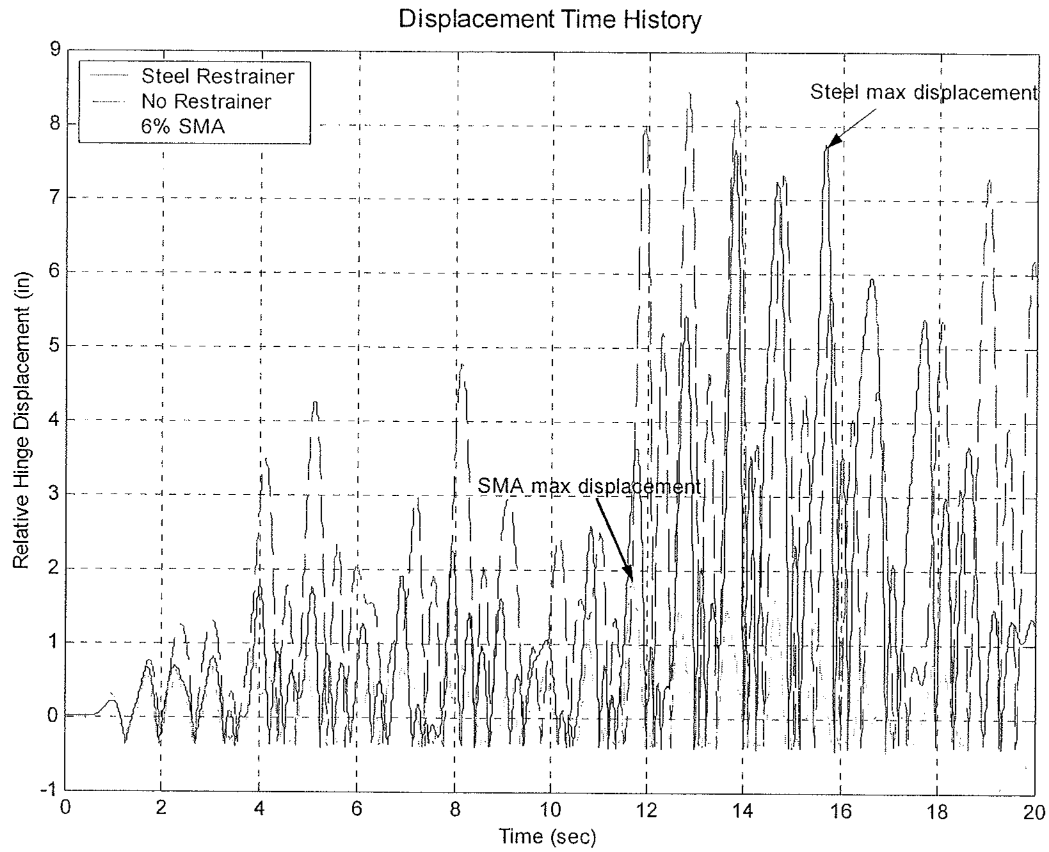

Figure 28. Analytical results for time history of relative hinge displacement (Case II)

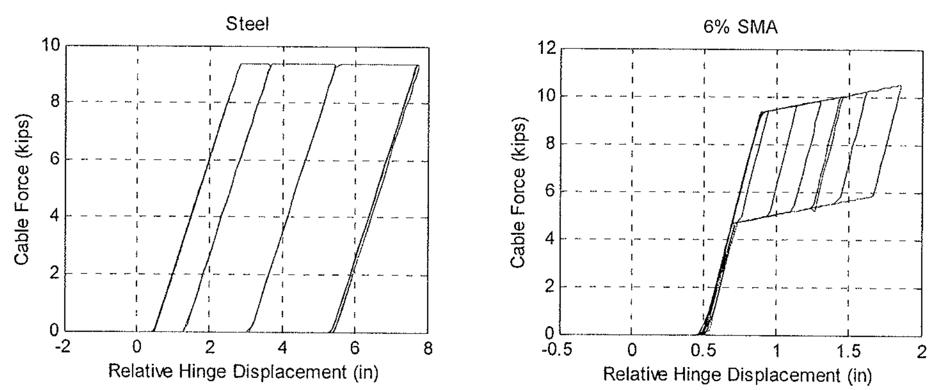

Figure 29. Analytical results for force-displacement of steel cable restrainers and SMA cable restrainers (Case II)

	Max Hinge Displacement	*Max Cable Force*
	CASE II	
SMA Restrainer	2.76 in (70.1 mm)	7.33 Kips (32.5 kN)
Steel Restrainer	3.90 in (99.0 mm)	5.62 Kips (24.9 kN)
	CASE III	
SMA Restrainer	1.86 in (47.2 mm)	10.5 Kips (46.7 kN)
Steel Restrainer	7.76 in (197 mm)	9.38 Kips (41.6 kN)

Table 5. Summary of results of preliminary analytical study

Experimental Testing of Seismic Performance of NiTi SMA Bridge Restrainers

A series of tests were conducted at the UNR Large Structures Laboratory, in cooperation with Georgia Institute of Technology, to determine experimentally, the effects of shape memory alloy (SMA) cable restrainers on the seismic performance of in-span hinges of a representative multiple-frame concrete box girder bridge subjected to earthquake excitation. Another objective of this study was to compare the performance of SMA to steel restrainers as restraining devices to reduce hinge displacements and reduce the likelihood of unseating of frames at the hinge during seismic activity. The data collected from SMA restrainer experiments was compared to information gathered in a previous UNR study on the performance of traditional steel restrainers (Sanchez-Camargo et al 2004). A preliminary analysis was performed at Georgia Tech to predict the performance of SMA restrainers using ground motions previously used during the steel restrainer studies at UNR. A simple 2-DOF model was used in the design of the SMA restrainers using a worst-case scenario from the previous steel restrainer experiments. During testing two types of SMA cables were used. The smaller of the SMA restrainers had a collective stiffness of 420 kN/m (2.4kip/in) and zero slack while the larger of the SMA cables had a collective stiffness of 700 kN/m (4.0 kip/in) and a restrainer slack of 12.7mm. (0.5 in.) (Johnson et al 2004). Figure 30 shows a close-up of an SMA cable restrainer.

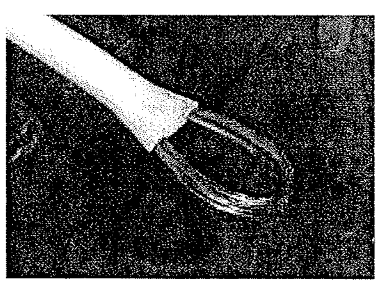

Figure 30. SMA cable restrainer

Parameters of Experimental Study

This section presents the parameters used in this study. They are the same parameters as those used in the comparable steel restrainer studies (Sanchez-Camargo et al 2004). The worst-case scenario from the previous UNR experiments in which the steel restrainers either had significant displacements or failed also established the parameters of study used in the SMA restrainer experiments. These parameters helped provide the criteria for the SMA restrainer design and test protocol. They include the following:

(a) A frame period ratio of 0.6 between the two adjacent bridge frames was determined to result in large out-of-phase motions. This ratio between the structural periods is taken as the period of the stiffer frame (the frame producing less movement during dynamic motion) over the period of the more flexible frame (the adjacent frame producing more movement).

(b) Restrainer stiffness is another important parameter. Table 6 shows the properties of two sets of restrainer systems. Each set consists of steel cable restrainers and "equivalent" SMA cable restrainers that have the same stiffness as the steel restrainers. In the first set each cable system has a stiffness equal to 73.5 k/in (0.42 kN/mm) and in the second, each system has stiffness equal to 123 k/in (0.7 kN/mm). The stiffness of the restrainers was determined based on geometric properties (length and cross-sectional area), material properties (modulus of elasticity), and number of cables used. The 6% strain that was used for the basis of the design stiffness of the restrainers was also used in the calculation of the chord modulus.

(c) Restrainer slack, the amount of displacement which takes place before the restrainers engage, was another important parameter during the SMA restrainer shake table tests. Two different values of restrainer slack, 12.7 mm (1/2 in) and 0 mm (0 in) were used. As in the earlier steel restrainer tests, zero slack was used for the restrainer with a stiffness of 73.5 k/in (0.42 kN/mm), while a slack of 0.50 in (12.7 mm) was used for the stiffer (0.7 kN/mm) SMA cables. These combinations of slack and stiffness produced the maximum responses in the case of the steel restrainers.

(d) The earthquake input motion was a synthetic Applied Technology Council ATC32-E (soft soil) (California Department of Transportation 2001) based on a design spectrum for Caltrans. It is based on expected magnitude of earthquake (6.5), soil type of the site (E or soft soil), and peak ground acceleration (PGA). Past steel restrainer experiments utilizing various soil types, determined soil type E to be an important factor in producing the large out of phase motion that resulted in frequent restrainer engagement during shake table testing. Peak ground accelerations between 0.05g and 0.25g with 0.05g increments were selected.

RESTRAINER CABLES PARAMETERS	Steel	84-wire SMA
Number of Restrainers	**3**	**2**
Size of Restrainers (diameter)	3.175mm (1/8 in)	84x0.584mm (84x0.023in)
Area of Restrainers (total)	11.6 mm^2 (0.018in^2)	45.2 mm^2 (0.07 in^2)
Restrainer Length	3.95 m (155.5 in)	1159 mm (45.625 in)
Modulus of Elasticity	146757 MPa (21300 ksi)	31716 MPa (4600 ksi)
Chord Modulus Calculated at 6% Strain		10756 MPa (1560 ksi)
Restrainer Stiffness (K)	0.42 kN/mm (2.4 kip/in)	0.42 kN/mm (2.4 kip/in)
	Steel	**130-wire SMA**
Number of Restrainers	**5**	**2**
Size of Restrainers (diameter)	3.175mm (1/8 in)	130x0.584mm (130x0.023in)
Area of Restrainers (total)	19.35 mm^2 (0.03in^2)	75.23 mm^2 (0.1166 in^2)
Restrainer Length	3.95 m (155.5 in)	1155 mm (45.475 in)
Modulus of Elasticity	146757 MPa (21300 ksi)	34474 MPa (5000 ksi)
Chord Modulus Calculated at 6% Strain		11721 MPa (1700 ksi)
Restrainer Stiffness (K)	0.7 kN/mm (4.0 kip/in)	0.7 kN/mm (4.0 kip/in)

Table 6. Restrainer Cable Parameters, Steel vs. SMA

Test Specimen and Experimental Process

The test specimen, seen in Figure 31, was designed during the UNR steel restrainer experiments (Vlassis et al 2000, Sanchez-Camargo 2004) and is intended to simulate an in-span hinge within a multi-span concrete box girder bridge. Dimensions of the specimen were based on superstructure dimensions of representative Caltrans bridges. The box girder cells used typify the end part of the frames at expansion joints. Block A, seen as the right block in Fig. 31d, is the lighter of the concrete cells, with a mass of 0.787 kg (0.054 slugs) while Block B, the left block in Fig 31d, with additional lead added, is the heavier cell with a mass of 1.09 kg (0.075 slugs). Elastomeric bearing pads, seen in Fig. 31c, simulating the substructure stiffness, were attached between the bottom of the box girder cells and the shake table, seating the lighter of the frames over the stiffer pads, with a collective stiffness of 1303 kN/m (7.44 kip/in,) and the heavier of the frames (the cell supplemented with lead bricks) over the less stiff pads, with a collective stiffness of 683 kN/m (3.9 kip/in). This resulted in the block period ratio of 0.6 discussed above. The individual frame periods of 0.53 and 0.87 were accomplished with the addition of lead bricks to the hollow concrete cells. The individual block properties with the resulting period ratio of 0.6 are presented in Table 7.

Individual Block Properties	Block A		Block B	
Weight of Block	(92.5 kN)	20.8 kip	(93.9 kN)	21.1 kips
Weight of Additional Lead	0	0	(34.5 kN)	7.75 kips
Weight of Block + Additonal Lead	(92.5 kN)	20.8 kip	(128.3 kN)	28.85 kip
Mass of Block + Additional Lead	(.787 kg)	0.054 slug	(1.09 kg)	0.075 slug
Measured Stiffness from 4 Elastomeric Bearings	(1303 kN/m)	7.44 k/in	(683 kN/m)	3.90 k/in
Frequency of Vibration (□)	11.74 rad/sec		7.21 rad/sec	
Period of Block	0.53 sec		0.87 sec	
T_A/T_B	0.6			

Table 7. Block properties

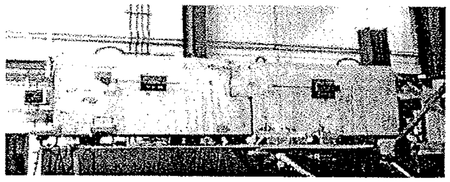

(a) SMA Shake Table Test Set-Up

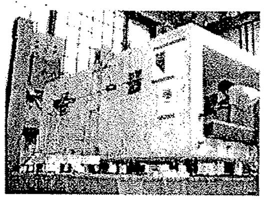

(b) Additional Lead in Block (c) Elastomeric Bearing Pad

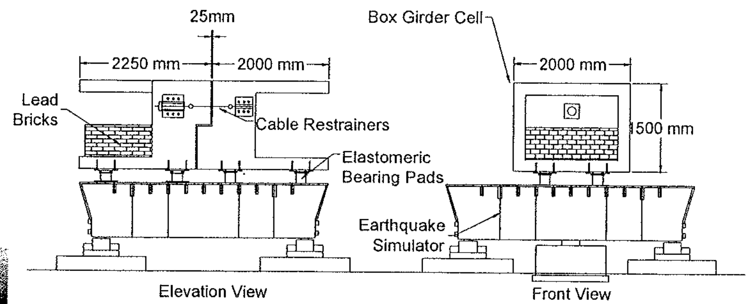

(d) Block and Bearing System Design

Figure 31. Experimental test set-up representing multi-frame concrete box girder bridge

The SMA restrainers were attached to the frames using steel mountings, seen in Figure 32. Two distinct attachment plates were formed for the east and west side of the model. Both sets of plates were made with a steel strength of 248 MPa (36 ksi) and were designed to be bolted through both sides of each frame element. The wires of the looped end of the SMA cables were spread over a 19.05 mm (3/4") diameter steel pin that was part of a yoke system that was welded to one side of the plates. A piece of leather was placed between the steel pin and cable ends to act as a stress reliever and prevent cutting action on the wires that could lead to early failure. The larger of the plates held the load cell to detect force in the restrainers.

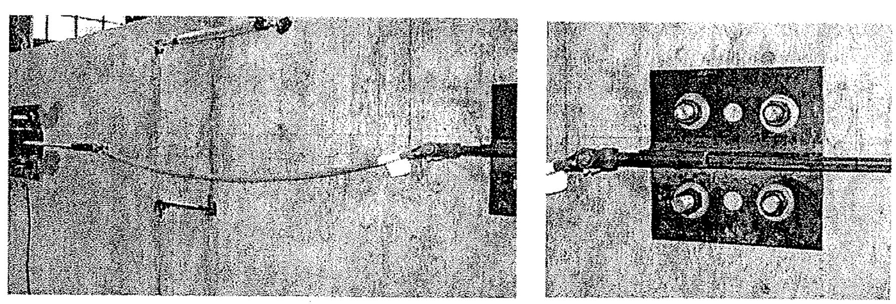

Figure 32. Steel mountings for connecting SMA restrainer to frame

The experiment was performed on one of the 50-ton capacity biaxial shake tables at UNR. Three linear displacement transducers were placed on the east, west and topside of the hinge section. These three displacement transducers (LWG-225 Novotechnik) seen in Fig. 33 directly measured the relative displacement at the hinge. Absolute displacement of the blocks was measured with two Unimeasure String Potentiometers.

These instruments measured the displacement between the specimen and a fixed frame. Accelerometers centrally located on the blocks evaluated impact forces and a load cell measured the force on the restrainers. Figure 33 shows the complete instrumentation plan.

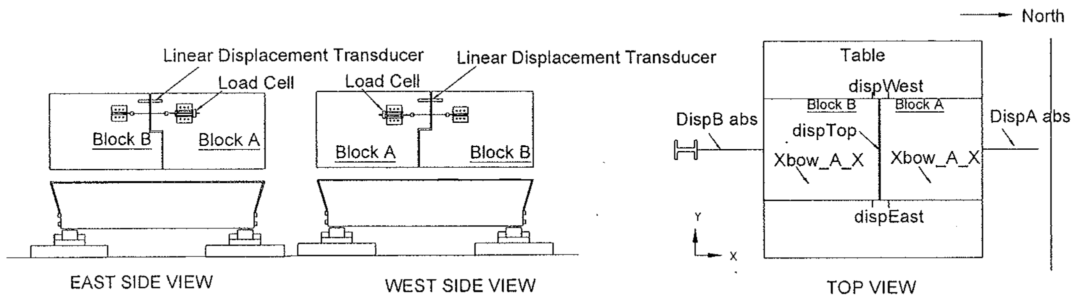

Figure 33. Instrumentation for data collection

Experimental Results – SMA Restrainers

Table 8 shows the peak displacement and maximum forces that were recorded during the shake table tests as well as the calculated stress-strains. Because of space limitations in this article, only the information from the east-side restrainer is displayed in Table 8 (see Fig. 33). The recorded hinge displacement for the larger SMA cable includes the initial 0.50 in (12.7 mm) slack. The first column of the table shows the run number. Case 1, 2 and 3 are SMA restrainer shake table runs that are directly equivalent to the previous steel restrainer experiments. These runs were used for comparing the behavior of the SMA and steel cable restrainers. Relative displacement between the blocks was generated in output files from the data acquisition system. Increasing displacement was noted with escalating ground accelerations.

Run	PGA	SMA Cable size	Slack (mm)	Slack (in)	Peak Disp (mm)	Peak Disp (in)	Cable Strain (%)	Max Force (kN)	Max Force (kip)	Max Cable Stress (MPa)	Max Cable Stress (ksi)
84-1	0.05g	84-wire	0	0	9.5	0.37	0.81	4.6	1.04	206.4	29.9
84-2	0.10g	84-wire	0	0	15.8	0.62	1.35	8.4	1.89	373.1	54.1
84-3 **(case1)**	0.15g	84-wire	0	0	23.0	0.91	1.97	10.5	2.35	464.9	67.4
84-4	0.20g	84-wire	0	0	28.4	1.12	2.43	11.1	2.49	492.1	71.4
84-5	0.25g	84-wire	0	0	37.2	1.46	3.18	11.0	2.47	487.4	70.7
130-1	0.05g	130-wire	12.7	0.5	21.2	0.83	0.72	4.7	1.05	134.4	19.5
130-2	0.10g	130-wire	12.7	0.5	28.7	1.13	1.37	12.0	2.70	344.6	50.0
130-3 **(case 2)**	0.15g	130-wire	12.7	0.5	32.1	1.26	1.66	17.5	3.94	503.1	73.0
130-4 **(case 3)**	0.20g	130-wire	12.7	0.5	38.9	1.53	2.25	18.9	4.24	541.8	78.6
130-5	0.25g	130-wire	12.7	0.5	45.2	1.78	2.78	18.8	4.23	539.6	78.3

Table 8. Peak displacements and maximum forces for east-side restrainer

SMA Stress-Strain Relationship

Figures 34(a) through Fig. 34(c) are all part of the same shake table test with incremental increases of ground acceleration of 0.5g. Figure 34 illustrates the stress-strain relationships for the 84-wire cable for run 84-3, with a PGA of 0.15g, to run 84-5, with a PGA of 0.25g. The superelastic effect of this material is evident in these graphs. It shows the ability of this material, NiTi, to go through repeated deformation cycles with minimal accumulation of residual strain. The recentering ability of the SMA is most visible at the larger accelerations. At the maximum PGA of 0.25g, seen in Fig. 34(c), the stress of the 84-wire cable is approximately 483 MPa (70 ksi) and the corresponding strain is approximately 3%. The usable strain range of this material is 6-8%. In Fig. 34(a), with a PGA of 0.15g, a maximum stress of 465 MPa (67.4 ksi) and a corresponding strain of 1.97% were reached. Run 84-4, seen in Fig. 6(b), with increased acceleration amplitude of 0.2g, shows an opening of the hysteretic loop that is characteristic of the superelastic effect of SMA. The maximum stress and strain associated with a PGA of 0.2g are 492 MPa (71.4 ksi) and 2.43%, respectively. Due to the large displacement of the elastomeric bearings, and the effectiveness of the SMAs in limiting the relative hinge displacement, a strain of 6% in the SMAs was not achieved during dynamic testing. The largest strain realized on the SMA restrainers during the test on the shake table was 3%, as seen in Fig. 34(c). Even at this 3% strain, the SMA hysteresis that results from its mechanical ability to recover deformation after stress removal is clearly evident in the typical flag shape loop that is synonymous with SMAs superelasticity.

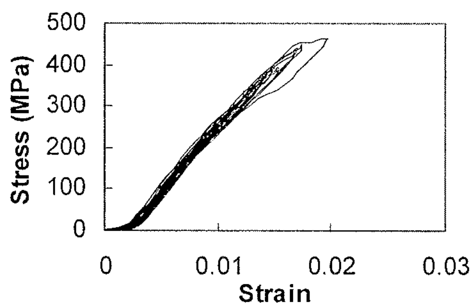

(a) 84-wire SMA Cable, PGA = 0.15g

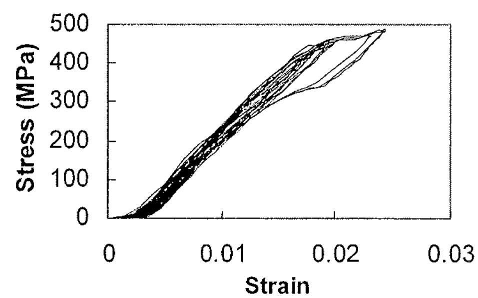

(b) 84-wire SMA Cable, PGA = 0.2g

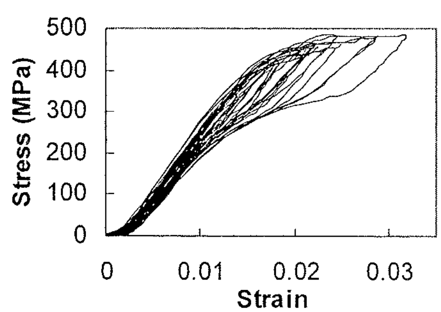

(c) 84-wire SMA Cable, PGA = 0.25g

Figure 34. Stress-strain relationships for SMA cable with increasing acceleration

A comparison, taken during shake table tests, of the relative hinge displacement between blocks and total restrainer force for both the 84-wire and 130-wire SMA cables at a PGA of 0.25g is illustrated in Fig. 35. The initial 12.7 mm (0.5 in) restrainer slack for the larger restrainer is seen as the point where the force in the large restrainer begins to increase. The relative hinge displacement, as viewed in Fig. 35, is larger for the 130-wire cable, but subtracting the initial 12.7 mm (0.5 in) slack gives a restrainer elongation of 32.5mm (1.28in) for the 130-wire cable vs. a restrainer elongation of 37.2 mm (1.46 in) for the smaller 84-wire cable restrainer. At a PGA of 0.25g, the force in the 84-wire SMA restrainer is 11 kN (2.5 kip) while the force in the 130-wire restrainer is almost 19 kN (4.3 kip). As in stress-strain relationships seen in Fig. 34, the force-displacement relationship seen in Fig. 35 reveals the recentering capabilities of SMA to return to its point of origin with minimal residual elongation.

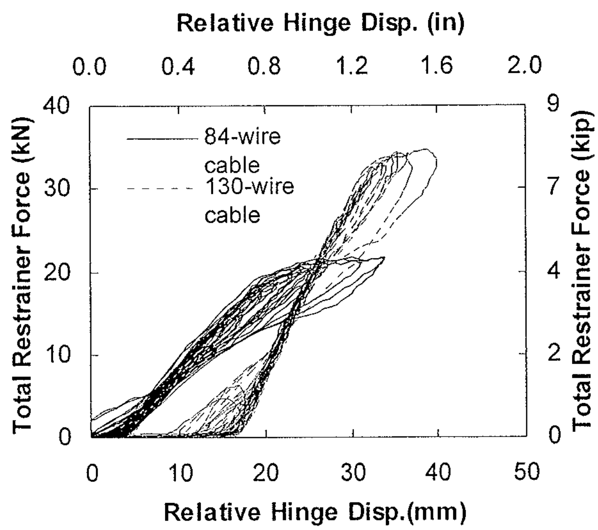

Figure 35. Force-displacement for 84-wire cable and 130-wire cable

Experimental Results – SMA vs. Steel Restrainers

Comparison of SMA and Steel

As stated earlier, Binary NiTi SMAs appear to possess the properties desired in seismic resistant design and retrofit of structures. These properties, which include energy dissipation, large elastic strain capacity, hysteretic damping and re-centering capabilities are evident in the tests performed in this study. In order to evaluate the Nitinol restrainers in relation to the past research performed on steel restrainers with comparable stiffness, the test parameters above were duplicated. An overlay of earthquake response spectra of the steel and SMA tests revealed an equivalency between the dynamic steel and SMA restrainer tests for Case 1, 2 and 3. Figure 36 shows these response spectra with the 84-wire and 130-wire SMA cable at a PGA of 0.15g (Case 1 and 2), and the 130-wire cable at a PGA of 0.2g (Case 3).

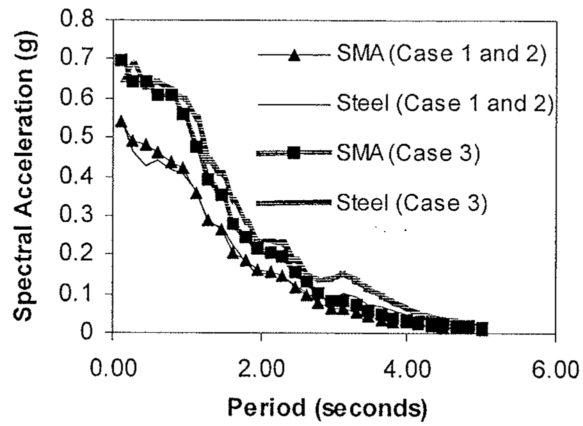

Figure 36. Response spectra for steel and SMA restrainers, Cases 1-3

SMA vs. Steel, Block Acceleration History

The acceleration history of Block B (the soft block) from the SMA experiment was compared to the Block B acceleration histories from the previous steel restrainer tests for Case 1, 2 and 3. During earthquake tests, all three equivalent cases produced lower acceleration in the blocks with SMA restrainers compared to those being restrained by steel. In Case 1, the maximum Block B acceleration for the SMA vs. steel restrainer shake table tests were 2.7g vs. 6.3 g., correspondingly. Figure 37 reveals similar results for Case 2 and 3. In Case 3, the acceleration in Block B resulting from earthquake motion in which steel restrained the blocks was more than 3.5 times larger (11.6g vs. 3.2g) than the block acceleration in which SMA was the restraining device.

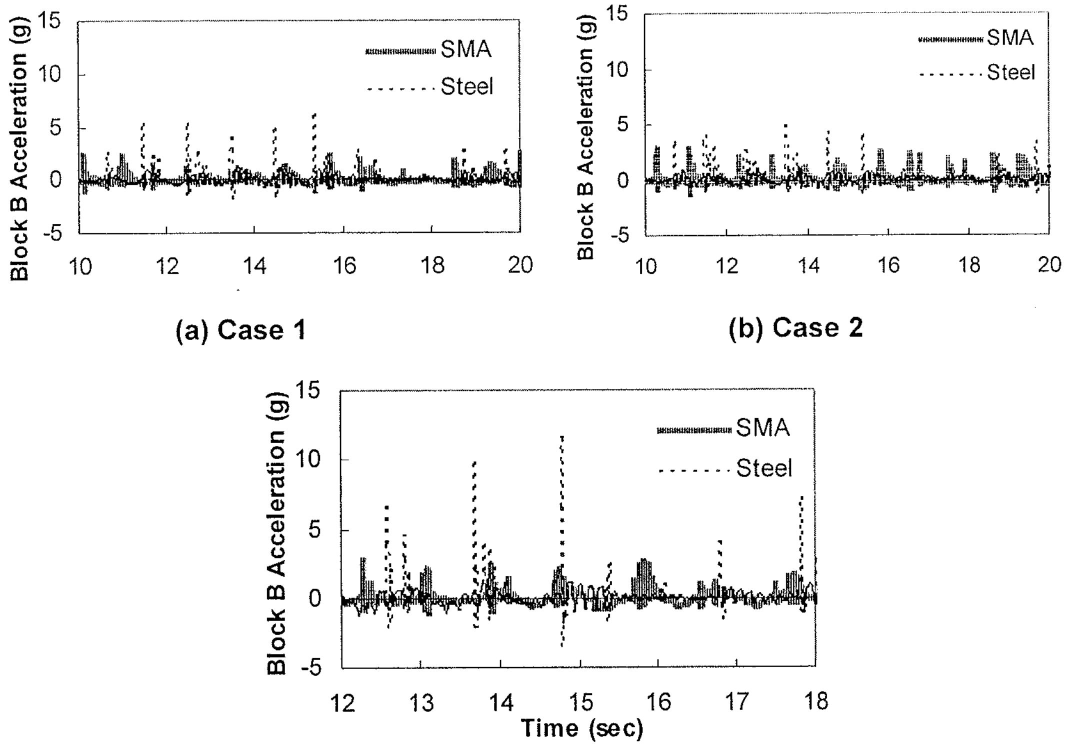

(a) Case 1

(b) Case 2

(c) Case 3

Figure 37. Block accelerations for Cases 1-3

SMA vs. Steel, Force-Displacement

Figure 38 shows a graphical representation of the force displacement relationships for Case 1, 2, and 3 and its equivalent case from the past steel restrainer tests. Data was collected every 0.005 seconds during shake table testing for the 20-second dynamic test for the steel cable restrainer and the 38-second test for the SMA cable restrainer. The data collected during these experiments measuring maximum restrainer force and maximum relative hinge displacement for these three cases is shown in Table 4. The restrainer force-displacement relationships seen in Figure 38 reveals fairly equivalent steel and SMA restrainer force but larger relative hinge displacement with the steel restrainers. One can observe that the maximum hinge displacement for steel in Case 1 and 2 is nearly double that of the SMA restrainers. In Case 1, the 3-cable steel restrainer has elongated 43 mm (1.7 in) while the equivalent 84-wire SMA restrainer has an elongation of 23 mm (0.91 in). The maximum hinge displacement for the larger 5-cable steel restrainer and 130-wire SMA restrainer in Case 2 is 61 mm (2.39 in) and 32mm (1.26 in) respectively. As shown in Table 3, Cases 1 and 2 are at the equivalent earthquake motion of a PGA of 0.15g. Figure 10c reveals an extremely large relative hinge displacement in the 5-cable steel restrainer at a PGA of 0.2g. This figure shows that in Case 3, there was a restrainer failure in two of the five cables in the steel restrainer resulting in a maximum restrainer displacement more than three times larger in the steel vs. the SMA restrainer. The displacement of the steel cable restrainer in Case 3 is 120 mm (4.73 in) while that of the SMA cable restrainer is 39 mm (1.53 in).

Figure 38c also reveals that while the steel restrainer has failed, the SMA restrainer is just reaching yield beyond which the SMA can undergo large elastic deformation with reversibility.

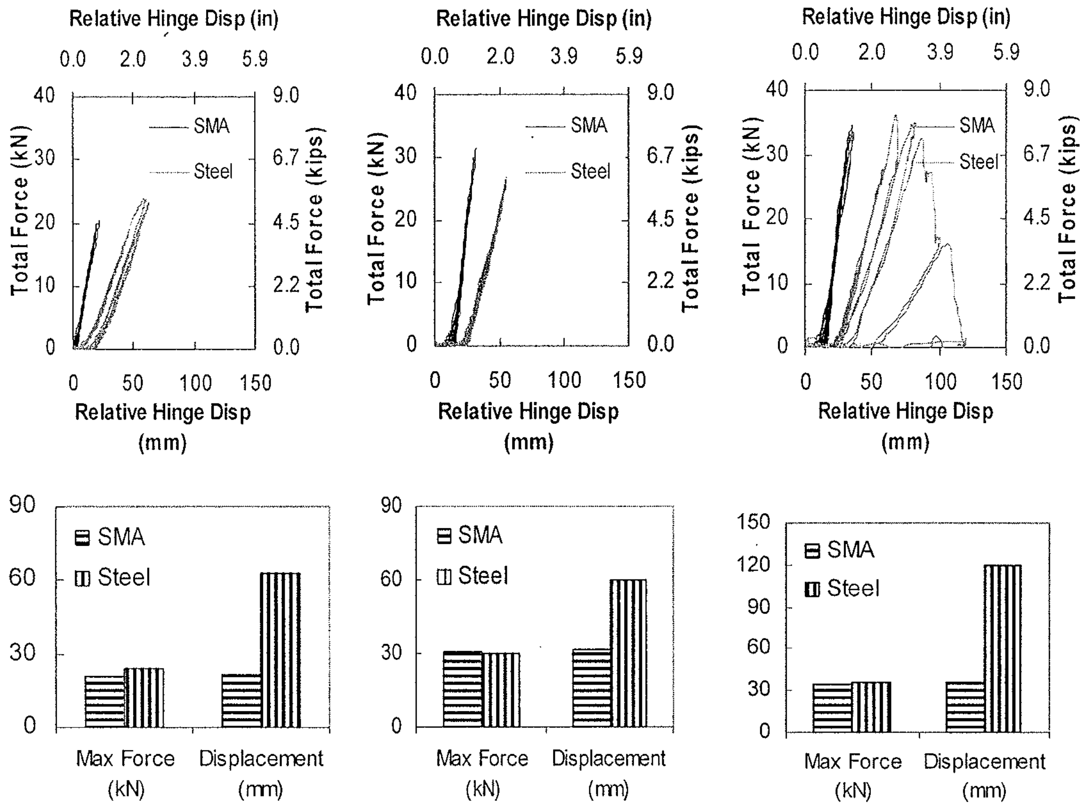

(a) Case 1 (b) Case 2 (c) Case 3

Figure 38. Force-displacements from tests of SMA and Steel restrainers

Summary and Conclusions from Experimental Study of SMA Restrainers

The objective of the experimental tests was to evaluate the seismic performance of shape memory alloy (SMA) as a retrofit or construction material for bridge restrainers and to compare their performance to the seismic performance of steel restrainers. The design of the SMA restrainers was based on data collected from steel restrainer experiments in an identical test setup that was performed in the large-scale structures laboratory at the University of Nevada, Reno. The tests were performed at incremental increases of ground motion on a shake table. The period ratio of 0.6, which resulted in an out-of-phase motion between the simulated single width box girder cells remained constant throughout the experiments. The tests utilized two identical SMA restrainers, one on either side of the specimen. A 3% strain was realized in the cables under dynamic loading and the SMA cables displayed the hysteretic damping and energy dissipation associated with superelastic shape memory alloys.

The following conclusions can be drawn from the results of this experimental study:

1. The SMA restrainers were superior to the steel restrainers in limiting relative hinge displacements. Maximum hinge displacements using the SMA restrainers were less than one-half of those using the steel cable restrainers for the same input motion. This would reduce the possibility of unseating of the frames at the in-span hinge of bridges during seismic activity.

2. With equivalent restrainers, under identical earthquake motion, the steel restrainer failed while the SMA restrainers only reached their yield level.

3. SMA restrainers produce lower block accelerations during earthquake excitation compared to experiments with equivalent steel restrainers. The energy associated with the phase transformation of SMA from the austenite to martensite results in higher restrainer energy dissipation and lower energy transfer to the structure.

4. The forces in the SMA and steel restrainers were comparable. This demonstrates that the SMA restrainers can withstand forces equal to or greater than those of traditional steel bridge restrainers.

5. The SMA cable restrainers had minimal residual strain after repeated cycling. Unlike steel, SMA can undergo many cycles of loading with little degradation of properties.

Cost Analysis

A cost analysis is conducted to determine the feasibility of using SMA restrainers in place of traditional steel restrainer cables. The same methodology used in the design of the restrainer cables (Page 26) is used in determining the cost. The design of the SMA cables is based on having the same strength, and stiffness of a **5-ft (1.52 m), 0.22 in^2** steel restrainer cable commonly used in bridge retrofit. While a larger cross section area is required for the SMA (due to the difference in strength with steel), a much shorter length is needed, due to the large elastic strain range. A **16 inch (406 mm), 0.80 in^2 (51.6 mm^2) area SMA cable** or rod, provides the same stiffness and strength as the 5 ft (1.52 m) high strength steel restrainer cable. Such as cable would have a material cost of approximately $500 dollars. When you include manufacturing and associated hardware, and heat treatment, the cost per cable would be approximately $850 dollars. A recently completed retrofit project performed by the TN DOT used 5 – ft high strength steel restrainer cables. The cost of each cable, including attachments was approximately $750 (Ed Wasserman and Wayne Seager, *Personal Communication*). The cost of the SMA cables is approximately 13.3% higher than that of the traditional steel cables. However, as noted in the study, the SMA cables provide much better performance in terms of reduction in relative high displacements, compared with steel restrainers. In fact, one can evaluated the potential of using significantly less SMAs to achieve the same performance as traditional cables. Also, the material costs of SMAs (approximately $50-$75 per pound) has decreased significantly in the past 5 years, and will continue to decrease as applications warranting large quantifies are identified. This will directly impact of the cost of the SMA cables.

Conclusions

This project evaluated the potential of using SMAs as restraining elements in bridges subjected to seismic loading. The study consisted of materials tests, detailed analytical studies, large-scale shake table tests, and cost analysis.

A detailed study was performed on the mechanical behavior of NiTiCr and NiTi under loadings typical of a seismic event. The results of an in-depth annealing study and strain rate study of NiTiCr and NiTi provided evidence into the proper annealing temperature to ensure the least amount of residual strain during cycling and thus providing the greatest recentering capability. This limits the hinge opening when used as restrainer cables for seismic rehabilitation in bridge systems. Further, the stress-strain behavior was obtained for both NiTiCr and NiTi undergoing a far field type loading protocol at strain rates of 0.5 Hz, 1.0 Hz, and 2.0 Hz. The results show a decrease in the residual strain with increased strain rate. Both types of SMAs also provided damping through their superelastic behavior.

In addition to material testing and identification of ideal treatment, an analytical study was performed to investigate the viability of NiTi SMA restraining devices in multi-frame bridges. Models of the SMA elements were developed based on past experimental studies. This study showed that the proposed superelastic elements are capable of reducing the relative hinge displacements in multiple frame bridges during strong ground motions without increasing the ductility demand on the bridge frames and thus preventing the unseating of the bridge superstructure. The superelastic elements reduced the relative hinge displacements significantly compared to the steel restrainers (30%-60% compared to steel restrainers). The response time history showed that during the first few cycles both types of restrainers perform similarly. Once the steel restrainers yield it begins accumulating residual strain and thus its effectiveness is reduced significantly. However, the SMA superelastic restrainers remain effective during the entire time history due to its capability to recenter and recovering its original length after being deformed to a level of strain that can reach 6%-8%.

The experimental investigation of NiTi SMA bridge restrainers offered key understanding of the performance of this class of SMA as unseating prevention devices. The testing performed in collaboration with UNR demonstrated that the SMA restrainers were superior to traditional steel restrainers in limiting relative hinge displacements, thus reducing the likelihood of unseating of the frames at in-span hinges during seismic activity. SMA restrainers were found to produce lower block accelerations, attributed to the energy dissipated during phase transformations of the SMA from the austenite to martensite phases. Additionally, minimal residual strain was observed in the SMA restrainers after repeated cycling, demonstrating the effectiveness of the superelastic nature of the material.

A cost analysis showed that SMA restrainers are 13.3% more expensive, compared to cost of traditional steel restrainer cables. However, the SMAs result in much better bridge performance, compared to steel cables. In addition, manufacturers of SMAs note that the prices will decrease as applications warranting significant quantities of SMAs are found.

Product Pay-Off Potential

There are thousands of bridges in the United States that are in need of seismic retrofit. The state of California alone has spent nearly $750 million in seismic retrofit since the 1989 Loma Prieta earthquake. Many other state DOT's are now beginning to initiate similar retrofit programs, including New York, Tennessee, Illinois, and South Carolina. While the cost of SMA restrainers is slightly higher than the cost of conventional steel restrainer retrofit, the benefits provided by SMA restrainers compared to traditional restrainers should be considered in the overall assessment of the cost-effectiveness of SMA restrainers. Factors that may dictate the cost-effectiveness of SMA restrainers include the hazard level of the bridge, the importance of the bridge, and expected performance of the bridge to various earthquakes.